agriculture

MDPI

Article

Effects of Compost Amendments on Soil Properties, Nematode Communities, and Physiological Performance of Jerusalem Artichoke (*Helianthus tuberosus* L.) in a Pot Experiment

Anita Zapałowska [1,*], Wacław Jarecki [2], Andrzej Tomasz Skwiercz [3], Dawid Kozacki [4] and Małgorzata Kunka [3]

[1] Department of Agriculture and Waste Management, University of Rzeszów, St. Ćwiklinskiej 1a, 35-601 Rzeszów, Poland
[2] Department of Crop Production, University of Rzeszów, St. Zelwerowicza 4, 35-601 Rzeszów, Poland; wjarecki@ur.edu.pl
[3] The National Institute of Horticultural Research, 96-100 Skierniewice, Poland; andrzej.skwiercz@inhort.pl (A.T.S.); malgorzata.kunka@inhort.pl (M.K.)
[4] Institute of of Biological Sciences, Cardinal Stefan Wyszyński University, Wóycickiego 1/3, 01-938 Warsaw, Poland; d.kozacki@uksw.edu.pl
* Correspondence: azapalowska@ur.edu.pl

Abstract

Organic amendments can influence plant growth through changes in both soil fertility and biological communities. However, the effects depend on the amendment type and substitution ratio. This study investigated how replacing peat with compost and vermicompost affected soil properties, nematode communities, and the growth and physiological performance of Jerusalem artichoke (*Helianthus tuberosus* L.). Seven treatments were compared: peat alone and peat containing 25%, 50%, or 75% compost or vermicompost. Treatment effects differed: 50% vermicompost (T6) resulted in the highest net photosynthetic rate, PSII efficiency, stem biomass, and tuber mass, whereas 75% compost (T4), despite having the highest nutrient concentrations, did not provide the best plant performance. These findings demonstrate that nutrient enrichment alone does not determine plant responses and highlight the importance of considering growing-medium properties and nematode communities when evaluating organic amendments.

Keywords: agricultural management; soil food web; trophic groups; organic amendments; soil health; soil–plant interactions

Check for updates

Academic Editor: Riccardo Scotti

Received: 17 September 2026
Revised: 21 October 2026
Accepted: 16 November 2026
Published: 18 November 2026

Copyright: © 2026 by the authors. Licensee MDPI, Basel, Switzerland. This article is an open access article distributed under the terms and conditions of the Creative Commons Attribution (CC BY) license.

1. Introduction

In modern agriculture, the intensive use of mineral fertilizers poses significant risks to soil biota and overall soil health [1,2]. Studies have shown that long-term chemical fertilization can decrease the diversity and richness of soil microbial communities [3,4]. Consequently, there is an urgent need to transition toward circular economy practices, such as the application of organic amendments, including composts, which contribute to waste valorization and soil carbon sequestration [5]. Properly managed compost amendments improve soil physical and chemical properties by enhancing organic matter content and increasing the availability of essential macronutrients—such as nitrogen (N), phosphorus (P), and potassium (K)—directly boosting plant growth and crop yields [6–8]. Soil health is defined as the capacity of soil to function as a living ecosystem that sustains productivity, biodiversity, and the provision of ecosystem services in terrestrial ecosystems. Unlike

traditional approaches focused primarily on soil fertility and chemical properties, the soil health concept emphasizes the central role of soil biota in maintaining essential ecological functions. In this context, bioindicators are valuable tools for monitoring and understanding biologically mediated soil processes, including the maintenance of soil structure, organic matter decomposition, cycling of key elements such as carbon, nitrogen, and phosphorus, and the natural regulation of organism populations. Soils provide essential ecosystem services, including carbon sequestration, nutrient cycling, organic matter decomposition, water storage, and the regulation of pests and pathogens [9].

Because soil processes are governed by complex interactions that vary spatially and temporally, biological indicators are increasingly used to assess soil health, as they reflect the combined effects of multiple environmental factors. Among soil fauna, nematodes are considered particularly valuable indicators of soil condition because their communities respond to changes in environmental conditions and food-web functioning [10,11]. Kapp et al. [12] highlighted the potential of nematode communities as indicators of soil health, while Knox et al. [13] demonstrated that nematode movement in heavy clay soils is restricted, suggesting that soil physical properties may influence their distribution. In addition to these physical constraints, soil biological communities are affected by nutrient management practices. For example, Xu et al. [3] reported that long-term chemical fertilization can reduce soil bacterial diversity, whereas Li et al. [4] found that long-term chemical and organic fertilization can increase soil multifunctionality, although these practices differentially affect microbial associations. Such findings highlight the complexity of soil responses to fertilization and the importance of considering multiple biological indicators when evaluating soil condition. In this context, nematode trophic groups are particularly useful because their different feeding habits and functional roles allow them to respond differently to changes in resource availability and environmental disturbance, making them sensitive indicators of soil conditions and soil food-web functioning [14–19].

Soil nematode communities and food web indices can inform about the complexity, nutrient flows and decomposition pathways of soil food webs, reflecting soil quality. Bacterivorous and fungivorous nematodes participate in nutrient cycling, while omnivorous and predatory groups provide information about the structure and complexity of the soil food web. Plant-parasitic nematodes, in turn, may reflect potential biological constraints on plant growth. Therefore, nematode community composition and ecological indices can complement physicochemical soil analyses when assessing the effects of organic amendments.

Relative abundance of nematode feeding and life-history groups are used for calculating food web indices, i.e., maturity index (MI), enrichment index (EI), structure index (SI) and channel index (CI) [20]. Jerusalem artichoke (*Helianthus tuberosus* L.), a perennial asteraceous crop prized for its high tuber yield, inulin content, and bioenergy potential, requires sustainable cultivation strategies that optimize biomass production while maintaining long-term soil ecological integrity. In modern agriculture, the intensive use of mineral fertilizers poses significant risks to soil biota and overall soil health [21].

While the chemical properties of composts are well-documented, their physiological benefits to crops are largely mediated by the belowground soil micro-food web.

Despite the recognized benefits of organic amendments, the interactive effects of compost quality and dosage on the growth parameters of *Helianthus tuberosus* L. and the simultaneous response of the rhizosphere micro-food web require deeper elucidation.

The aim of this study was to investigate the effects of different peat substitution ratios with compost and vermicompost on the growth and yield of Jerusalem artichoke (*Helianthus tuberosus* L.), the physicochemical properties of the growing substrate, and nematode community structure under controlled pot conditions. Particular emphasis was placed on examining the relationships between substrate properties, nema-

tode community characteristics, and plant physiological responses to different organic amendment treatments.

2. Materials and Methods

2.1. Experimental Materials

Three growing materials were used: compost, vermicompost, and peat substrate.

The compost was a solid organic fertilizer produced from biodegradable organic waste. The raw materials used for its production included mainly green waste, such as plant residues, branches, grass, and leaves. According to the product specification, the compost contained 0.7% total nitrogen (N), 0.8% phosphorus expressed as P_2O_5, and 0.3% potassium expressed as K_2O. The organic matter content in dry matter was 40%.

The vermicompost was characterized by a slightly alkaline reaction (pH 7.0). Its nutrient content was 200 mg·kg^{-1} N-NO_3, 68.7 mg·kg^{-1} N-NH_4, 617 mg·kg^{-1} P, 1795 mg·kg^{-1} K, 1410 mg·kg^{-1} Ca, 369 mg·kg^{-1} Mg, and 189 mg·kg^{-1} Cl. The organic carbon (Corg) content was 5.08%.

Peat substrate was used as the reference growing medium. It was slightly acidic (pH 6.4) and had a salinity of 0.6. The substrate contained 2.6 mg·kg^{-1} N-NO_3, 0.01 mg·kg^{-1} N-NH_4, 16.6 mg·kg^{-1} P, 40.6 mg·kg^{-1} K, 1227 mg·kg^{-1} Ca, 201 mg·kg^{-1} Mg, 92 mg·kg^{-1} Na, 96 mg·kg^{-1} S-SO_4, and 80 mg·kg^{-1} Cl. The concentrations of Fe, Mn, Cu, Zn, and B were 251, 0.4, 0.3, 1.13, and 0.29 mg·kg^{-1}, respectively. The Corg content was 38%, total N was 1.78%, and the C:N ratio was 22.09.

Jerusalem artichoke (*Helianthus tuberosus* L.) tubers of the 'Gigant' cultivar were used as planting material (Figure 1).

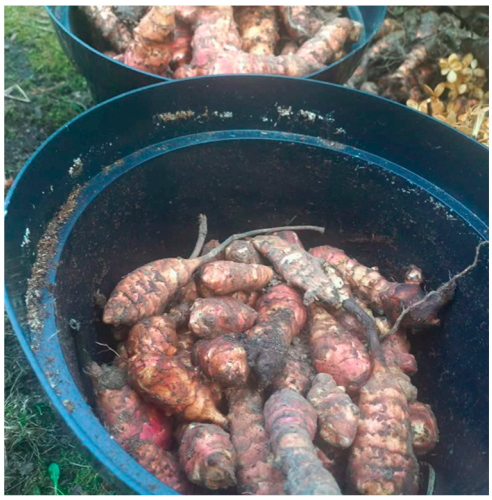


Figure 1. Jerusalem artichoke (*Helianthus tuberosus* L.) tubers used in experiment.

The experimental treatments were established by mixing the peat substrate with different proportions of compost or vermicompost. The following seven treatments were used:

- T (1)—control treatment consisting of peat substrate (100% peat substrate);
- T (2)—peat substrate amended with 25% compost (25% compost + 75% peat substrate);
- T (3)—peat substrate amended with 50% compost (50% compost + 50% peat substrate);
- T (4)—peat substrate amended with 75% compost (75% compost + 25% peat substrate);
- T (5)—peat substrate amended with 25% vermicompost (25% vermicompost + 75% peat substrate);
- T (6)—peat substrate amended with 50% vermicompost (50% vermicompost + 50% peat substrate);

- T (7)—peat substrate amended with 75% vermicompost (75% vermicompost + 25% peat substrate).

A pot experiment was conducted using the prepared substrates in 5 L pots, with one *Helianthus tuberosus* L. tuber planted at a depth of 1 cm in each pot. The experimental design included three replicates for each treatment, comprising two compost variants applied at four different rates. The experiment was initiated in April 2026 and conducted for 7 consecutive weeks at the Plant Production Laboratory of the University of Rzeszów under controlled conditions with supplemental LED lighting. The plants were grown at an air temperature of 20 ± 2 °C and a relative humidity of 70 ± 3%. A 16/8 h light/dark photoperiod was maintained throughout the experiment, with a maximum photosynthetic photon flux density of approximately 300 µmol m^{-2} s^{-1}. Temperature and relative humidity were continuously monitored throughout the 24 h cycle. Substrate moisture was maintained at 60% of the maximum water-holding capacity (MWHC) to provide a stable and moderately moist growing environment. Three independent replicates were used for each treatment.

2.2. Substrate Analysis

Chemical properties, including pH, salinity expressed as total dissolved salts, and the concentrations of plant-available nutrients, were assessed using a standardized universal analytical procedure [22]. Readily available nitrogen (N–NO_3 and N–NH_4), phosphorus (P), potassium (K), magnesium (Mg), and calcium (Ca) were extracted with 0.03 N acetic acid at a substrate to-extractant ratio of 1:10 (v/v). Nitrate and ammonium concentrations in the resulting extracts were determined potentiometrically using ion-selective electrodes (Thermo Scientific, Waltham, MA, USA; NO_3^- electrode, model 93-07; NH_4^+ electrode, model 93-1801), whereas phosphorus was quantified using a colorimetric method.

The remaining macronutrients were quantified by atomic absorption spectroscopy (AAS; Thermo Electron Corp., M Series, Waltham, MA, USA). Measurements were performed at characteristic wavelengths of 766.5 nm for K, 285.2 nm for Mg, 422.9 nm for Ca, and 589.0 nm for Na using a hollow-cathode lamp. The concentrations of the remaining elements were determined by inductively coupled plasma optical emission spectrometry (ICP-OES; PerkinElmer OPTIMA 2000 DV, PerkinElmer Inc., Waltham, MA, USA), with each element analyzed at its characteristic emission wavelength [23–27]. Organic matter content was determined by dry combustion in a muffle furnace at 550 °C and expressed as a percentage of dry matter (% DM).

Organic carbon content (Corg) was calculated from the organic matter content using the conversion factor reported in [28].

2.3. Plant Physiological Characteristics

Chlorophyll a fluorescence was measured using a Pocket PEA portable fluorimeter (Hansatech Instruments, King's Lynn, Norfolk, UK). Measurements were performed on four fully developed, healthy leaves per pot at a comparable developmental stage. Prior to measurement, leaves were dark-adapted for 30 min using specialized leaf clips to ensure that the PSII reaction centers were fully open. Fluorescence transients were recorded for 1 s under red excitation light with a peak wavelength of 627 nm and a maximum light intensity of 3500 µmol PAR m^{-2} s^{-1}. The maximum quantum yield of PSII photochemistry (Fv/Fm), variable-to-minimum fluorescence ratio (Fv/F0), time to maximum fluorescence (Tfm), and the area above the fluorescence induction curve (Area, expressed in bms) were determined from the recorded fluorescence transients. Parameters were calculated automatically using Pocket PEA software based on fast chlorophyll a fluorescence induction kinetics.

Gas-exchange measurements were conducted using an LCpro-SD portable photosynthesis system (ADC BioScientific Ltd., Herts, UK). Measurements were performed on

two fully developed, healthy leaves per pot under standardized conditions. The photosynthetic photon flux density inside the measurement chamber was maintained at 1500 µmol m^{-2} s^{-1}, and chamber temperature was set to 22 °C. Leaves were allowed to equilibrate in the chamber until stable measurement conditions were reached. Net photosynthetic rate (A), stomatal conductance (Gs), and transpiration rate (E) were recorded. Net photosynthesis was expressed as µmol CO_2 m^{-2} s^{-1}, whereas stomatal conductance and transpiration were expressed as mmol H_2O m^{-2} s^{-1}. Leaf temperature (Tleaf) was recorded during gas-exchange measurements and expressed in °C.

Leaf area was measured using digital image analysis with Easy Leaf Area [29]. Photographs of leaves were taken and analyzed based on RGB pixel values to distinguish leaf tissue from the background. A red calibration area included in each image allowed automatic scaling, enabling precise calculation of leaf area (cm^2) without manual measurement. The software generated output files containing leaf area values for each analyzed image.

Plant height was measured as the length of the main shoot from the substrate surface to the apical meristem using a ruler with a precision of 1 mm. Measurements were taken at the end of the experiment for all plants in each treatment. The results are expressed in centimeters (cm) as mean values per treatment.

The biomass was determined using a RadWag WTB200 laboratory balance (RadWag, Radom, Poland). The results are expressed in grams. Both fresh and dry weights were measured. Fresh weight was recorded immediately after harvesting the plant material. Subsequently, the samples were dried in a drying chamber at 42 °C until a constant mass was achieved. The plant material was dried whole, without prior cutting. This procedure was applied consistently to all samples. After drying, the samples were cooled in a desiccator and weighed to determine dry biomass.

2.4. Nematode Isolation and Analysis

For each treatment, a composite substrate sample of 500 cm^3 was collected from the three pots. Nematodes were extracted from 500 cm^3 substrate samples using a modified centrifugation method according to Szczygieł [30]. Three 100 cm^3 subsamples per sample were processed, and the extracted nematodes were counted and identified based on morphological characteristics using the diagnostic keys of Brzeski [31] and Andrássy [32]. Nematodes were classified into five trophic groups: bacterivores, fungivores, plant-parasitic nematodes, omnivores, and predators. Population densities were expressed per 100 cm^3 of substrate. Identification and analysis followed Stefanovska et al. [33].

Briefly, 500 cm^3 of the collected substrate sample was mixed and separated into 100 cm^3 subsamples. The sediment suspension was transferred for centrifugation at 2000× *g* (RCF) for 3 min. The supernatant was discarded, and the precipitate was resuspended using 80 cm^3 of 1 molar sucrose solution.

The tubes were subjected to a final centrifugation at 2000× *g* (relative centrifugal force) for 2 min. The supernatant, containing the nematodes, was passed through a 25 µm sieve and rinsed three times with water to remove sucrose from the nematode bodies. The collected nematodes were then transferred to glass containers. To ensure thermal inactivation, the nematodes were treated with a 6% formalin solution at 90 °C, followed by fixation with an equal volume of water.

The isolated nematodes were transferred to a fixation container containing the S1 solution, which consisted of 20 cm^3 of 96% ethanol, 1 cm^3 of glycerol, and 79 cm^3 of distilled water. These containers were then placed in a desiccator with a thin layer of 96% ethanol and subsequently moved to an incubator at 40 °C. After 24 h in the desiccator, S2 solution-composed of 93 cm^3 of 96% ethanol and 7 cm^3 of glycerol-was gradually added to the

nematodes, with a few drops introduced each hour over 8 h. The nematodes were found to become fully saturated with glycerol after 24 h in the incubator.

For microscopic observation, nematodes embedded in glycerol were mounted on glass slides using drops of anhydrous glycerol, following the paraffin ring method. Identification was based on morphological characteristics, examined with a Carl Zeiss Jena A-Scope microscope and guided by the diagnostic keys of Brzeski [31] and Andrássy [32].

The following parameters of nematode communities were analysed: total abundance (number of individuals per 100 cm^3 of substrate), taxonomic composition at the genus level, trophic structure, community dominance, and diversity indices. Trophic structure was evaluated based on the relative proportions of five feeding guilds: bacterivores, fungivores, herbivores, omnivores, and predators [34]. Taxonomic diversity and community evenness were determined using taxon richness, the Shannon diversity index H' and Simpson's dominance index (D), which were calculated using PAST software (version 5.3) [35].

To assess the functional condition and structural complexity of the substrate food web, the following ecological indices were determined based on the colonizer–persister classification: Maturity Index (MI), and Plant Parasitic Index (PPI) [36]. The c-p classification groups nematode taxa according to their life-history characteristics and responses to environmental disturbance, with c-p 1 taxa representing fast-reproducing opportunists and higher c-p groups generally representing taxa with slower life histories and greater sensitivity to disturbance [36].

Food web diagnostic indices were calculated according to the nematode faunal analysis framework: the Enrichment Index (EI), reflecting resource availability and opportunistic bacterial-mediated decomposition; the Channel Index (CI), indicating the relative dominance of fungal versus bacterial decomposition pathways; the Structure Index (SI), reflecting food web complexity, and the presence of higher trophic levels; and the Basal Index (BI), representing a depleted or disturbed food web condition [37]. Additionally, total nematode biomass was evaluated. All functional and ecological indices were calculated using the online NINJA tool (Nematode Indicator Joint Analysis) [38].

2.5. Statistical Analysis

The results obtained in the experiment were tested to statistical analysis using Statistica 13.3.0 (TIBCO Software Inc., Palo Alto, CA, USA). The normality of data distribution was assessed using the Shapiro–Wilk test, and the homogeneity was verified using Levene's test. A one-way analysis of variance (ANOVA) was performed, Tukey's post hoc test was used to determine and verify the relationship at a significance level of $p \leq 0.05$. The F-statistic was used to evaluate the statistical significance of differences between groups. Multiple polynomial regression analysis was performed, and the False Discovery Rate (FDR) method was applied to adjust for multiple comparisons. Principal component analysis (PCA), based on the correlation matrix, was performed to investigate multivariate relationships among soil properties, plant traits, and nematode trophic groups and to identify the main gradients of variation within the dataset. The first two principal components were interpreted based on their contributions to the total variance and the distribution of variables in the ordination space.

3. Results

3.1. Chemical Properties of Substrates

The applied compost treatments resulted in pronounced differences in the chemical properties of the substrate.

The substrate pH ranged from 5.90 to 7.03 (Figure 2A). The highest value was recorded in T(4) (7.03), followed by T(2) and T(3), both with a pH of 6.90. The pH values in T(1)

and T(5) were 6.40 and 6.03, respectively, whereas the lowest values (5.90) were recorded in both T(6) and T(7).

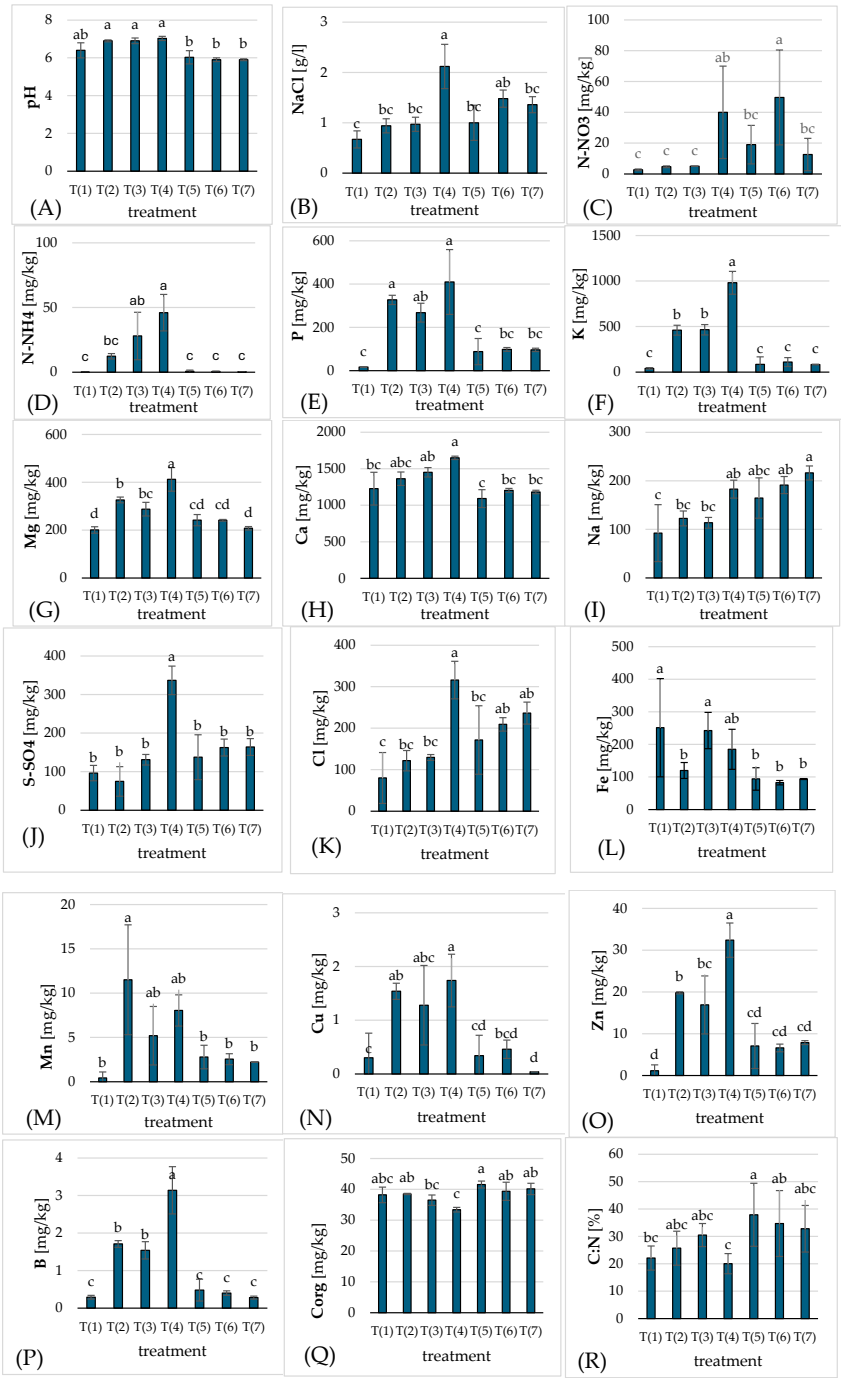


Figure 2. Effect of treatments (T1–T4) on substrate chemical properties: pH (**A**), salinity (**B**), nitrate (**C**), ammonium (**D**), phosphorus (**E**), potassium (**F**), magnesium (**G**), calcium (**H**), sodium (**I**), sulfates (**J**), chloride (**K**), iron (**L**), manganese (**M**), copper (**N**), zinc (**O**), boron (**P**), carbon (C) (**Q**), and C:N (**R**). Different letters indicate significant differences ($p < 0.05$) ($n = 3$). Bars represent standard deviation (SD).

Marked differences were also observed in the concentrations of mineral nitrogen forms. N-NO_3 ranged from 2.66 mg/kg in T(1) to 49.66 mg/kg in T(6), with particularly high values in T(4) (40 mg/kg) and T(6), while T(2), T(3) and T(7) showed substantially lower concentrations. In contrast, N-NH_4 displayed a distinct treatment pattern, reaching its

maximum in T(4) (46 mg/kg), followed by T(3) (28 mg/kg) and T(2) (12.3 mg/kg). Very low N-NH_4 concentrations were recorded in T(1), T(5), T(6) and T(7), ranging from 0.01 to 0.70 mg/kg (Figure 2C,D).

Phosphorus and potassium showed particularly pronounced differences among treatments. The highest P concentration was recorded in T(4) (410 mg/kg), followed by T(2) (327.33 mg/kg) and T(3) (268 mg/kg), whereas much lower values were observed in T(5)–T(7), ranging from 88.3 to 98.3 mg/kg. A similar pattern was observed for K, with the maximum concentration in T(4) (981 mg/kg), followed by T(3) and T(2) (465 and 460.3 mg/kg, respectively). In contrast, K concentrations in T(1), T(5), T(6) and T(7) were considerably lower, ranging from 40.6 to 110.3 mg/kg (Figure 2E,F).

Magnesium and calcium showed a less pronounced but still clear differentiation among treatments. Mg reached its highest concentration in T(4) (412.3 mg/kg), followed by T(2) (326.3 mg/kg) and T(3) (287.6 mg/kg), whereas the lowest values were recorded in T(1) and T(7) (201 mg/kg and 208 mg/kg, respectively). Calcium concentrations were highest in T(4) (1649.3 mg/kg), followed by T(3) (1451.3 mg/kg) and T(2) (1363.3 mg/kg). The lowest Ca concentration was observed in T(5) (1091.6 mg/kg), while T(6) and T(7) showed intermediate values (Figure 2G,H).

The concentrations of Na, S-SO_4 and Cl revealed another distinct treatment-related pattern. Na increased from 92.3 mg/kg in T(1) to 216.3 mg/kg in T(7), with relatively high values also observed in T(4) (183 mg/kg), T(5) (164.6 mg/kg) and T(6) (191.3 mg/kg). S-SO_4 and Cl showed their highest concentrations in T(4), reaching 337 mg/kg and 316 mg/kg, respectively. Considerably lower concentrations occurred in T(1) and T(2), whereas T(5)–T(7) showed intermediate values. This pattern was reflected in NaCl, which was highest in T(4) (2.12 mg/kg), compared with 0.67–1.48 mg/kg in the remaining treatments (Figure 2I,K).

The concentrations of Fe, Mn, Cu, Zn and B also varied considerably among the treatments. Fe showed the highest concentration in T(1) (251.3 mg/kg), with comparable values in T(3) (242.6 mg/kg), whereas the lowest concentrations were recorded in T(6) (82.5 mg/kg), T(7) (93.8 mg/kg) and T(5) (94 mg/kg). In contrast, Mn, Cu, Zn and B generally reached their highest values in T(4). Mn increased from 0.43 mg/kg in T(1) to 11.51 in T(2), with a value of 8.05 mg/kg in T(4), whereas T(5)–T(7) showed substantially lower concentrations. Cu ranged from 0.04 mg/kg in T(7) to 1.74 in T(4), while Zn ranged from 1.13 in T(1) to 32.40 in T(4). Boron showed a similar pattern, with the highest concentration in T(4) (3.14) and considerably lower values in T(1), T(5), T(6) and T(7) (Figure 2L,P).

Organic carbon (Corg) and C:N showed a contrasting distribution compared with many of the mineral nutrients. Corg ranged from 33.40 mg/kg in T(4) to 41.56 in T(5). The highest Corg concentration was therefore observed in T(5), followed by T(7) (40.13 mg/kg) and T(6) (39.36 mg/kg), whereas T(4) had the lowest value. T(1) and T(2) showed intermediate concentrations of 38.20 mg/kg and 38.50 mg/kg, respectively (Figure 2Q,R).

As the substitution ratio increased, the contents of NaCl, Ca^{2+}, and SO_4^{2-} also increased, indicating changes in the salt content of the substrate. Compared with compost, vermicompost did not significantly increase ammonium, boron, or other measured nutrients, while nitrate nitrogen content was higher, which may be relevant to potential nitrogen losses.

3.2. Physiological Parameters of Plants

Plant height and leaf area varied considerably among the compost treatments. Plant height ranged from 22.3 cm in T(1) to 40.6 cm in T(7), with a general increasing trend across treatments. The most pronounced increase was observed between T(4) and T(5), from 30.0 to 37.6 cm. Leaf area showed an even greater differentiation, ranging from 71.7 cm^2 in T(1) to 289.1 cm^2 in T(7). In contrast, T(5) showed a relatively large plant height (37.6 cm) but a comparatively low leaf area (113.3 cm^2) (Figures 3A,B and S1).

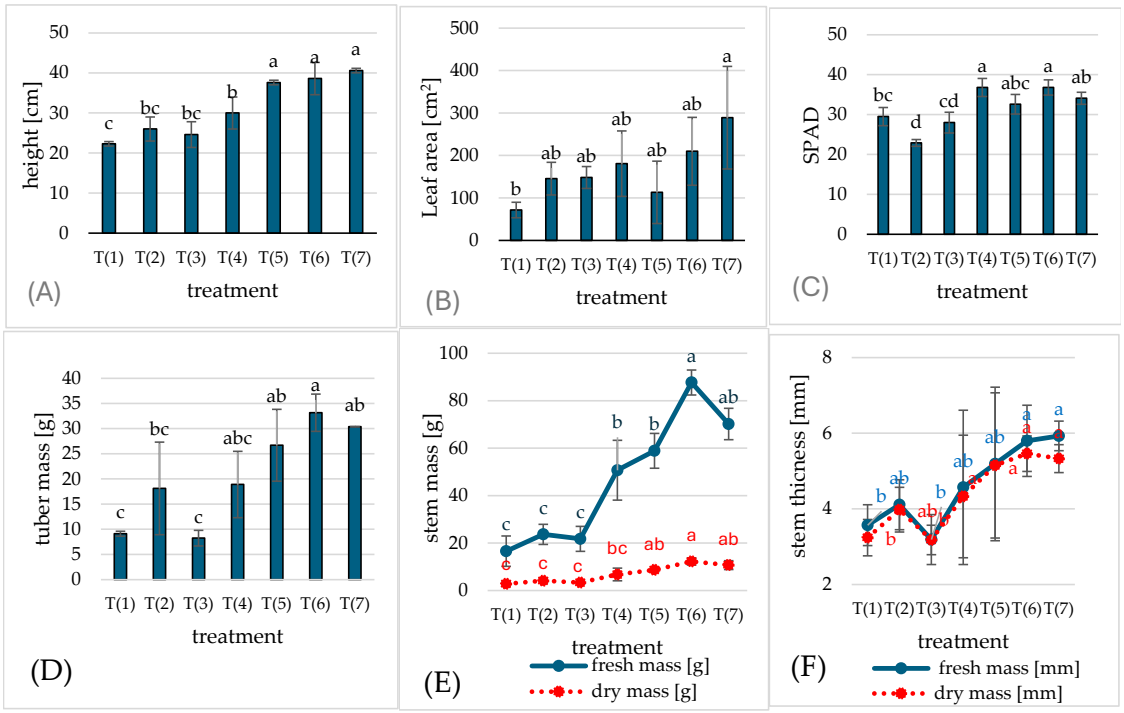


Figure 3. Effect of substrate treatments T(1)–T(7) on plant height [cm] (**A**), leaf area [cm^2] (**B**); chlorophyll contents [SPAD] (**C**), tuber mass [g] (**D**), stem mass [g] (**E**), stem thickness [mm] (**F**). Different letters indicate significant differences ($p < 0.05$), ($n = 3$). Bars represent standard deviation (SD).

SPAD values ranged from 22.9 in T(2) to 36.8 in T(4) and T(6) (Figure 3C).

Although T(7) produced the tallest plants and the largest leaf area, T(6) resulted in the highest tuber mass and stem biomass. The measured tuber biomass primarily represented the original tubers used as planting material. The final tuber mass varied considerably among the experimental treatments, ranging from 8.24 g in T(3) to 33.16 g in T(6) (Figure 3D).

Fresh stem mass increased from 16.6 g in T(1) to 87.7 g in T(6), accompanied by an increase in dry stem mass from 2.82 to 12.30 g (Figure 3E).

Stem diameter further differentiated the response of Jerusalem artichoke to the applied treatments. In fresh material, stem diameter increased from 3.57 mm in T(1) to 5.93 mm in T(7), with the lowest value recorded in T(3) (3.19 mm). A similar pattern was observed for the measurements associated with dry material, with stem diameter increasing from 3.24 mm in T(1) to a maximum of 5.46 mm in T(6), followed by a slightly lower value in T(7) (5.33 mm). The progressive increase in stem diameter from T(4) to T(7) coincided with increases in stem biomass and tuber mass, particularly in T(6) (Figure 3F).

The investigated treatments affected selected parameters of photosynthetic performance, particularly chlorophyll fluorescence characteristics, whereas the effects on gas-exchange parameters were less pronounced.

The maximum quantum yield of PSII photochemistry, expressed as Fv/Fm, differed significantly among treatments. The lowest Fv/Fm value was recorded in T(4) (0.772 ± 0.047), which was significantly lower than those observed in T(1) (0.825 ± 0.003), T(2) (0.821 ± 0.004), T(5) (0.831 ± 0.004), T(6) (0.832 ± 0.003), and T(7) (0.820 ± 0.007). Treatment T(3) (0.804 ± 0.030) showed an intermediate response and did not differ significantly from either group. The highest Fv/Fm values were observed in T(6) and T(5). The reduced Fv/Fm value in T(4) indicates lower maximum photochemical efficiency of PSII under this treatment compared with most of the other treatments.

A similar response pattern was observed for the variable-to-minimum fluorescence ratio (Fv/F0). The highest values were recorded in T(6) (4.966 ± 0.146) and T(5) (4.938 ± 0.159), whereas the lowest value was observed in T(4) (3.618 ± 0.826). The Fv/F0 value in T(4) was significantly lower than those recorded in T(5) and T(6), while the remaining treatments showed intermediate values and did not differ significantly from the other treatment groups. The consistent responses of Fv/Fm and Fv/F0 indicate comparatively lower PSII photochemical efficiency under T(4), whereas T(5) and T(6) maintained relatively high values of these fluorescence parameters.

The net photosynthetic rate (A) also varied among the treatments. The highest mean value was recorded in T(6) (15.72 ± 1.80 μmol CO_2 $m^{-2}s^{-1}$), whereas the lowest was observed in T(1) (6.47 ± 0.73 μmol CO_2 $m^{-2}s^{-1}$). The value recorded for T(6) was significantly higher than that for T(1), while the remaining treatments showed intermediate responses and did not differ significantly from either T(1) or T(6). The net photosynthetic rate in T(4) was relatively low (7.41 ± 1.29 μmol CO_2 $m^{-2}s^{-1}$); however, it did not differ significantly from the other treatments.

No significant differences among treatments were detected in stomatal conductance (Gs). Mean Gs values ranged from 0.10 ± 0.04 mmol H_2O m^{-2} s^{-1} in T(4) to 0.20 ± 0.03 mmol H_2O $m^{-2}s^{-1}$ in T(6). Although T6 exhibited the highest numerical Gs value, the lack of statistical significance indicates that the treatments did not significantly affect stomatal conductance.

Similarly, the transpiration rate (E) did not differ significantly among treatments. The highest numerical value was recorded in T(6) (4.43 ± 0.45 mmol H_2O $m^{-2}s^{-1}$), whereas the lowest was observed in T(3) (2.14 ± 0.43 mmol H_2O m^{-2} s^{-1}). The relatively high Gs and E values observed in T(6) occurred together with the highest net photosynthetic rate, suggesting comparatively active gas exchange under this treatment. However, because neither Gs nor E differed significantly among treatments, these differences should be considered numerical trends rather than statistically confirmed treatment effects.

Significant differences were observed in leaf temperature (Tleaf). Plants subjected to T(1) and T(2) exhibited significantly lower leaf temperatures (29.55 ± 0.67 and 29.58 ± 0.89 °C, respectively) than plants under T(3)–T(7), for which mean values ranged from 31.06 ± 0.28 to 31.95 ± 0.84 °C. These differences are relevant when interpreting the gas-exchange measurements because leaf temperature can influence stomatal behaviour, transpiration, and photosynthetic activity.

The area above the fluorescence curve (Area) also varied among treatments. The highest value was recorded in T(4) (543.106 ± 212.018 bms), whereas the lowest was observed in T(2) (289.022 ± 39.634 bms). T(4) exhibited a significantly higher Area than T(2), while the other treatments showed intermediate values and did not differ significantly from either treatment. The elevated Area in T(4), together with lower Fv/Fm and Fv/F0, does not indicate improved photosynthetic performance but rather an altered fluorescence induction response that should be interpreted alongside other chlorophyll fluorescence parameters.

The time required to reach maximum fluorescence (Tfm) differed significantly among treatments. The highest Tfm value was recorded in T(4) (707.5 ± 188 ms), which was significantly higher than those observed in T(1) (331.6 ± 52.4 ms), T(2) (333.3 ± 19.4 ms), T(5) (302.5 ± 9.0 ms), and T(7) (356.6 ± 26.7 ms). Treatments T(3) (473.3 ± 327 ms) and T(6) (445 ± 154 ms) showed intermediate values and did not differ significantly from the higher or lower groups. The markedly prolonged Tfm observed in T(4), together with its reduced Fv/Fm and Fv/F0 values, indicates an altered fluorescence induction kinetics under this treatment and is consistent with lower PSII photochemical efficiency.

T(4) showed the least favorable chlorophyll fluorescence response among the investigated treatments. This was particularly evident from its significantly lower Fv/Fm and

Fv/F0 values, together with the significantly prolonged Tfm and elevated Area. Although the net photosynthetic rate and stomatal conductance were also numerically lower in T(4), these differences were not statistically significant. In contrast, T(6) exhibited the most favorable overall photosynthetic characteristics, with the highest Fv/Fm, Fv/F0, and net photosynthetic rate, accompanied by numerically higher Gs and E values. These results indicates that T(6) was associated with efficient maintenance of PSII photochemical performance and relatively high photosynthetic activity (Table 1).

Table 1. Effects of substrate treatments T(1)–T(7) on photosynthetic performance (A, Gs, E) and chlorophyll fluorescence parameters (FV/Fm, Fv/F0, Tfm, area above the fluorescence curve) of Jerusalem artichoke (*Helianthus tuberosus* L.), mean ± SD, $n = 3$. Different letters indicate significant differences ($p < 0.05$).

Parameter	Treatments						
	T(1)	T(2)	T(3)	T(4)	T(5)	T(6)	T(7)
	Mean ± SD						
Maximum quantum yield of PSII photochemistry (FV/Fm)	0.825 ± 0.003 a	0.821 ± 0.004 a	0.804 ± 0.030 ab	0.772 ± 0.047 b	0.831 ± 0.004 a	0.832 ± 0.003 a	0.820 ± 0.007 a
Variable-to-minimum fluorescence ratio (Fv/F0)	4.732 ± 0.125 ab	4.589 ± 0.151 ab	4.190 ± 0.740 ab	3.618 ± 0.826 b	4.938 ± 0.159 a	4.966 ± 0.146 a	4.578 ± 0.235 ab
Net photosynthetic rate A [µmol [CO_2 m^2 s^{-1}]	6.47 ± 0.73 b	9.19 ± 6.17 ab	8.07 ± 1.59 ab	7.41 ± 1.29 ab	9.70 ± 1.18 ab	15.72 ± 1.80 a	12.84 ± 4.90 ab
Stomatal conductance Gs [mmol [H_2O m^{-2} s^{-1}]	0.12 ± 0.02 a	0.15 ± 0.12 a	0.11 ± 0.04 a	0.10 ± 0.04 a	0.18 ± 0.02 a	0.2 ± 0.03 a	0.16 ± 0.09 a
Transpiration rate E [mmol [H_2O m^{-2} s^{-1}]	2.66 ± 0.19 a	2.96 ± 1.39 a	2.14 ± 0.43 a	2.88 ± 0.91 a	4.04 ± 0.46 a	4.43 ± 0.45 a	3.54 ± 1.35 a
Tleaf [° C]	29.55 ± 0.67 b	29.58 ± 0.89 b	31.95 ± 0.84 a	31.83 ± 0.23 a	31.06 ± 0.28 a	31.35 ± 0.32 a	31.85 ± 1.56 a
Area above the fluorescence curve [bms]	318,907 ± 21,622 ab	289,022 ± 39,634 b	347,397 ± 108,813 ab	543,106 ± 212,018 a	357,670 ± 26,228 ab	435,469 ± 3724 ab	315,838 ± 28,117 ab
Time to reach maximum fluorescenceTfm [ms]	331.6 ± 52.4 b	333.3 ± 19.4 b	473.3 ± 327 ab	707.5 ± 188 a	302.5 ± 9 b	445 ± 154 ab	356.6 ± 26.7 b

The Fv/Fm parameter showed predominantly negative correlations with the analysed chemical properties of the substrate. The strongest negative association was found for ammonium nitrogen (N-NH_4; r = −0.775, $p = 0.0001$), followed by K (r = −0.707, $p = 0.0001$), B (r = −0.628, $p = 0.002$), *p* (r = −0.620, $p = 0.003$), and Zn (r = −0.601, $p = 0.04$). Moderate negative correlations were observed for Ca (r = −0.591, $p = 0.05$), Mg (r = −0.553, $p = 0.09$), S-SO_4 (r = −0.516, $p = 0.017$), NaCl (r = −0.498, $p = 0.022$), Cl (r = −0.488, $p = 0.025$), Cu (r = −0.484, $p = 0.026$), and pH (r = −0.463, $p = 0.035$), whereas weaker relationships were found for N-NO_3 (r = −0.370, $p = 0.099$), Mn (r = −0.318, $p = 0.160$), and Fe (r = −0.274, $p = 0.229$). In contrast, organic carbon content (C org) was positively correlated with Fv/Fm (r = 0.634, $p = 0.002$). The particularly strong negative relationship with N-NH_4, together with the positive association with C org, highlights a contrasting relationship between substrate organic matter status, ammonium availability, and PSII performance (Figure 4).

The gas-exchange parameters exhibited distinct relationships with substrate chemical properties. Both transpiration rate (E) and CO_2 assimilation rate (A) were negatively correlated with pH (r = −0.574 and r = −0.527, respectively), whereas positive correlations were observed with nitrate nitrogen (N-NO_3; r = 0.467 for E and r = 0.443 for A). E also showed a negative correlation with Fe (r = −0.494). In contrast, stomatal conductance (gs) showed no significant correlations with the analysed substrate parameters. Overall, the results suggest that substrate pH and the form of available nitrogen were among the factors most closely associated with photosynthetic CO_2 assimilation and transpiration in *Heliatnus tuberosus* L. plants. The linear regression analysis showed that soil variables influenced

plant physiological parameters to varying degrees. The coefficients of determination (R^2) for the analyzed variable pairs ranged from values close to zero to a maximum of 32% (Table 2).

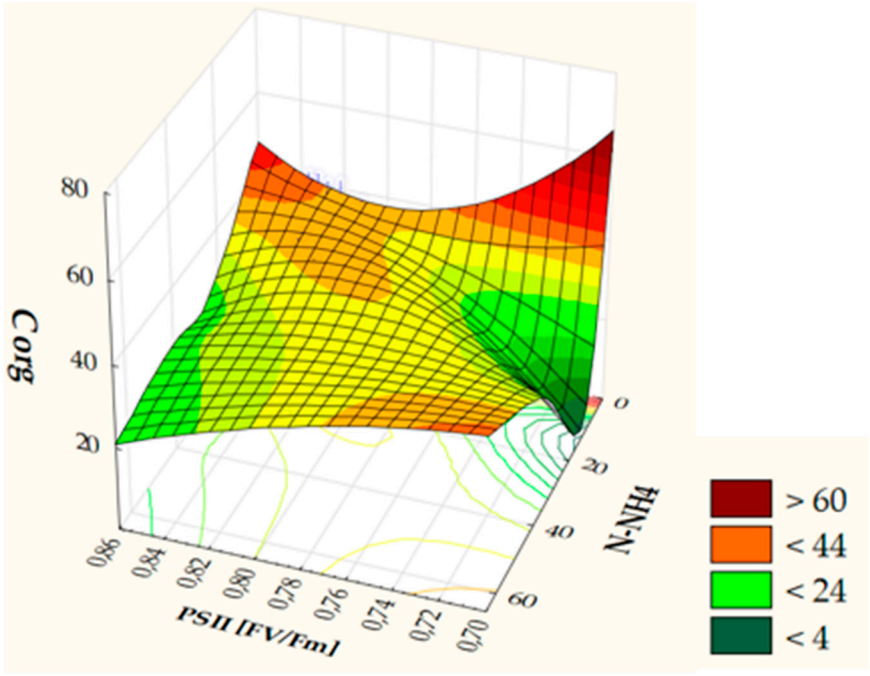


Figure 4. Surface regression model plots for Corg, PSII [FV/Fm] and N-NH_4.

Table 2. Relationships between soil chemical properties and plant physiological responses using the Benjamini–Hochberg false discovery rate (FDR) procedure.

Parameter	Transpiration Rate E [mmol [H_2O m^{-2} s^{-1}]		Stomatal Conductance Gs [mmol [H_2O m^{-2} s^{-1}]		Net Photosynthetic Rate A [µmol [CO_2 m^{-2} s^{-1}]	
	p	p B-H	p	p B-H	p	p B-H
pH	0.006	0.102	0.082	0.102	0.014	0.238
NaCl [g/l]	0.278	0.386	0.962	0.386	0.377	0.458
N-NO_3 [mg/kg]	0.033	0.187	0.248	0.187	0.044	0.3
N-NH_4 [mg/kg]	0.212	0.357	0.209	0.357	0.183	0.38
P [mg/kg]	0.067	0.265	0.141	0.285	0.245	0.383
K [mg/kg]	0.157	0.357	0.143	0.357	0.142	0.38
Mg [mg/kg]	0.365	0.443	0.307	0.443	0.201	0.38
Ca [mg/kg]	0.136	0.357	0.264	0.357	0.268	0.383
Na [mg/kg]	0.078	0.265	0.482	0.265	0.080	0.34
S-SO_4 [mg/kg]	0.987	0.987	0.284	0.987	0.645	0.685
Cl [mg/kg]	0.408	0.462	0.842	0.462	0.436	0.494
Fe [mg/kg]	0.023	0.187	0.107	0.187	0.053	0.3
Mn [mg/kg]	0.934	0.987	0.441	0.992	0.962	0.962
Cu [mg/kg]	0.231	0.357	0.420	0.357	0.179	0.38
Zn [mg/kg]	0.295	0.386	0.325	0.386	0.270	0.383
B [mg/kg]	0.194	0.357	0.197	0.357	0.125	0.38
Corg [mg/kg]	0.216	0.357	0.253	0.357	0.310	0.405

Correlation analyses were performed to assess the relationships between soil chemical properties and plant physiological parameters, including transpiration rate (E), stomatal

conductance (Gs), and net photosynthetic rate (A). To account for multiple testing, *p*-values were adjusted using the Benjamini–Hochberg false discovery rate (FDR) procedure, applied separately to each physiological parameter across 17 soil variables. Although several correlations showed nominal statistical significance ($p < 0.05$), none remained statistically significant after FDR correction (adjusted $p > 0.05$) (Table 2).

3.3. Nematodes Analysis

Analysis of nematode communities revealed distinct patterns across trophic groups, including plant-parasitic nematodes (PPNs), bacterivores, fungivores, omnivores, and predators (Figure 5).

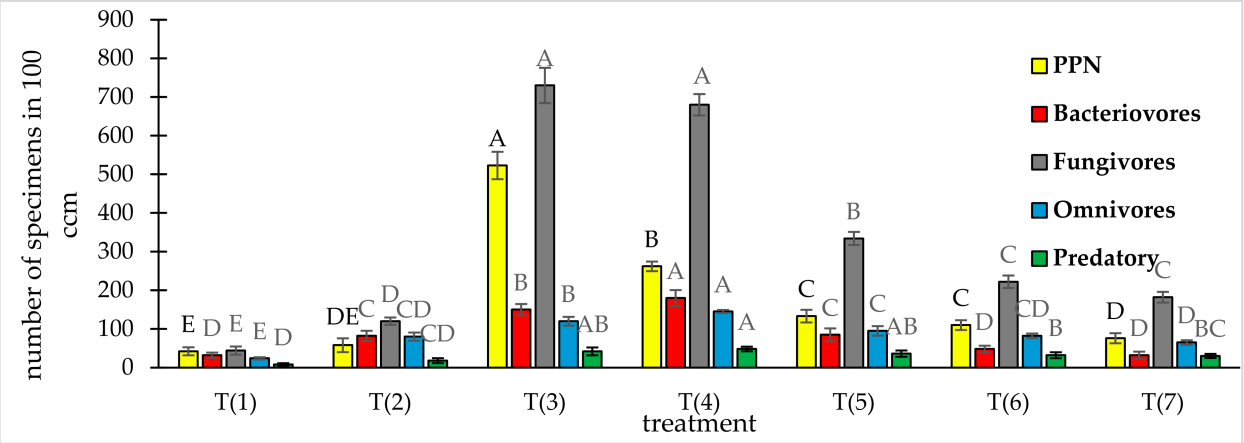


Figure 5. The abundance of five trophic groups (PPNs, bacterivores, fungivores, omnivores, and predators) expressed as the number of specimens per 100 cm^3 of substrates across the treatments T(1)–T(7). Capital letters indicate significant differences among the trophic groups of nematodes (PPN, bacterivores, fungivores, omnivores, and predators) within treatments T(1)–T(7), as determined by ANOVA followed by Tukey's HSD test ($n = 3$, $p \leq 0.05$).

The abundance of nematode trophic groups varied considerably among treatments. The highest abundance of plant-parasitic nematodes (PPNs) was recorded in T(3) (523 individuals), followed by T(4) (262 individuals),and T(5) (133 individuals) whereas the lowest abundance was observed in T(1) (42 individuals). Bacterivorous nematode abundance varied among treatments, ranging from 32 individuals in both T(1) and T(7) to 180 individuals in T(4). The abundance was 82 individuals in T(2), 150 in T(3), 85 in T(5), and 48 in T(6). Omnivores reached their highest abundance in T(4) (145 individuals) and their lowest in T(1) (24 individuals). Predatory nematodes were most abundant in T(4) (48 individuals) and least abundant in T(1) (8 individuals).

For the PPN (plant-parasitic nematodes),the highest abundance of *Coslenchus* was recorded in sample T(3), where it reached 480 individuals, while in sample T(4) it amounted to 210 individuals. In the remaining samples, the abundance of this genus was lower, but still exceeded the values recorded for *Pratylenchus*, *Merlinius*, *Rotylenchus*, and *Paratylenchus*. The highest abundance of *Pratylenchus* was observed in treatments T(3) and T(4) (12 individuals), while the lowest was recorded in T(7) (4 individuals). For *Merlinius*, the highest abundance was recorded in T(3) and T(4) (18 individuals), whereas the lowest occurred in T(2) (4 individuals). The abundance of *Rotylenchus* was highest in T(4) (20 individuals) and lowest in T(1) (5 individuals). *Paratylenchus* showed the lowest overall abundance, ranging from 2 individuals in T(4) to 6 individuals in T(6) and T(7) (Figure 6A).

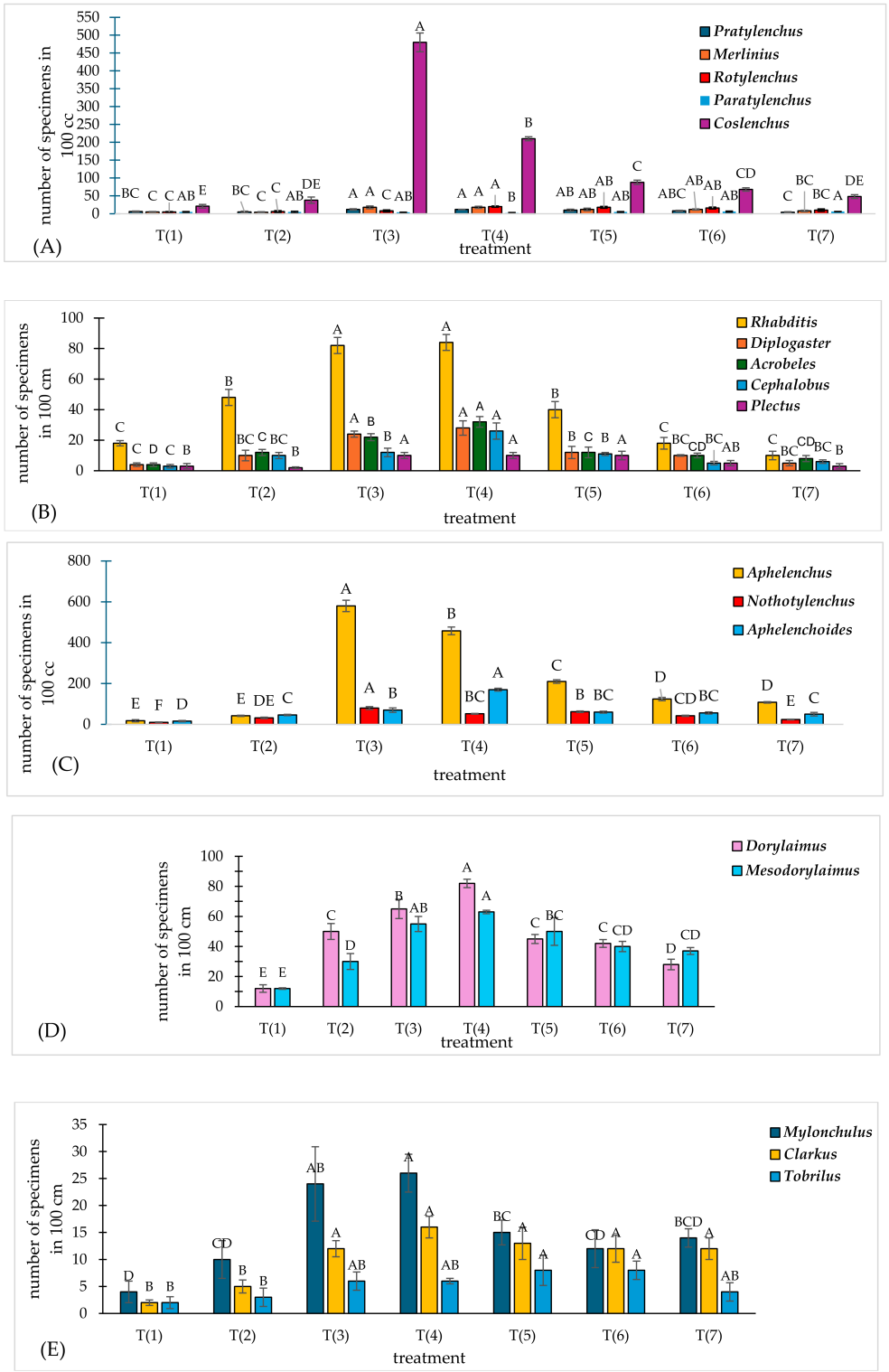


Figure 6. The abundance of five trophic groups: PPNs (**A**), Bacteriovores (**B**), Fungivores (**C**), Omnivores (**D**), Predators (**E**), expressed as the number of specimens per 100 cm^3 of substrates across the treatments T(1)–T(7). Capital letters indicate significant differences among individuals of PPNs (**A**), Bacteriovores (**B**), Fungivores (**C**), Omnivores (**D**), and Predators (**E**) within treatments T(1)–T(7), as determined by ANOVA followed by Tukey's HSD test ($n = 3$, $p \leq 0.05$). Bars represent standard deviation (SD).

The abundance of bacterivorous nematodes varied among treatments. *Rhabditis* was the most abundant genus, with the highest values recorded in T(4) (84 individuals) and T(3) (82 individuals), whereas the lowest abundance was observed in T(7) (10 individu-

als). *Diplogaster* reached its highest abundance in T(4) (28 individuals), followed by T(3) (24 individuals), while the lowest value was recorded in T(1) (4 individuals). The abundance of *Acrobeles* was highest in T(4) (32 individuals) and lowest in T(1) (4 individuals). *Cephalobus* showed a similar pattern, with the highest abundance in T(4) (26 individuals) and the lowest in T(1) (3 individuals). *Plectus* reached its highest abundance in T(3)–T(5) (10 individuals), whereas the lowest abundance was recorded in T(2) (2 individuals) (Figure 6B).

Fungivorous nematodes constituted the most abundant trophic group, particularly in T(3) and T(4). Their abundance increased from T(1) (65 individuals) to a maximum of 1210 individuals in T(3). This pattern was mainly driven by *Aphelenchus*, which reached 580 individuals in T(3), *Nothotylenchus* also attained its highest abundance in T(3) (80 individuals), whereas *Aphelenchoides* was most numerous in T(4) (170 individuals) (Figure 6C).

Omnivorous nematodes also exhibited their greatest abundance in T(4), reaching 145 individuals, compared with only 24 individuals in T(1). Within this trophic group, *Dorylaimus* and *Mesodorylaimus* showed comparable treatment-related patterns, attaining maximum abundances of 82 and 63 individuals, respectively, in T(4) (Figure 6D).

Predatory nematodes occurred at lower densities but displayed a clear treatment-related pattern. Their total abundance increased from 8 individuals in T(1) to 48 individuals in T(4). *Mylonchulus* and *Clarkus* reached maximum abundances in T(4) (26 and 16 individuals, respectively), whereas *Tobrilus* attained its highest density in T(5) and T(6) (8 individuals) (Figure 6E).

Treatment-related changes in nematode community structure are presented in Table 3 and Figure 7. Bacterivorous taxa demonstrated rapid demographic expansion primarily driven by bacterial-feeding enrichment opportunists (c-p 1). Among free-living nematodes, c-p 2 taxa predominated in all treatments, reaching the highest relative abundance in T(3) (74.30 ± 0.66%). In contrast, c-p 1 taxa declined progressively from 20.13 ± 1.37% in T(1) to 5.60 ± 1.74% in T(7). The abundance of c-p 4 taxa varied among treatments, with the lowest proportion recorded in T(3) (14.90 ± 0.32%) and higher values in T6–T7. The c-p 3 group remained minor (<2%), while c-p 5 taxa were absent.

Table 3. Relative abundance (%) of nematodes in colonizer-persister (CP 1–5) and plant-parasitic (PP 2–5) groups across treatments T(1)–T (7), (mean ± sd, $n = 3$).

Class	Treatment						
	T(1)	**T(2)**	**T(3)**	**T(4)**	**T(5)**	**T(6)**	**T(7)**
CP 1, % of free-living	20.13 ± 1.37	19.30 ± 2.02	10.1 ± 0.25	10.6 ± 0.5	9.4 ± 1.35	6.53 ± 1.23	5.6 ± 1.74
CP 2, % of free-living	50.10 ± 0.98	48.10 ± 3.7	74.3 ± 0.66	71.03 ± 0.47	66.76 ± 0.91	62.7 ± 1.75	64.4 ± 0.61
CP 3, % of free-living	1.53 ± 1.01	1.00 ± 0.69	0.60 ± 0.17	0.53 ± 0.06	1.50 ± 0.44	1.86 ± 0.84	1.50 ± 0.50
CP 4, % of free-living	28.2 ± 2.31	31.56 ± 2.67	14.9 ± 0.32	17.76 ± 0.42	22.33 ± 1.59	28.86 ± 1.76	28.43 ± 2.21
CP 5, % of free-living	-	-	-	-	-	-	-
PP 2, % of herbivores	61.56 ± 1.81	72.7 ± 3.32	92.6 ± 1.51	80.9 ± 2.09	69.86 ± 0.72	68.16 ± 1.75	69.8 ± 5.15
PP 3, % of herbivores	38.4 ± 1.81	27.3 ± 3.32	7.4 ± 1.51	19.1 ± 2.09	30.13 ± 0.72	31.83 ± 1.75	30.2 ± 5.15
PP 4, % of herbivores	-	-	-	-	-	-	-
PP 5, % of herbivores	-	-	-	-	-	-	-

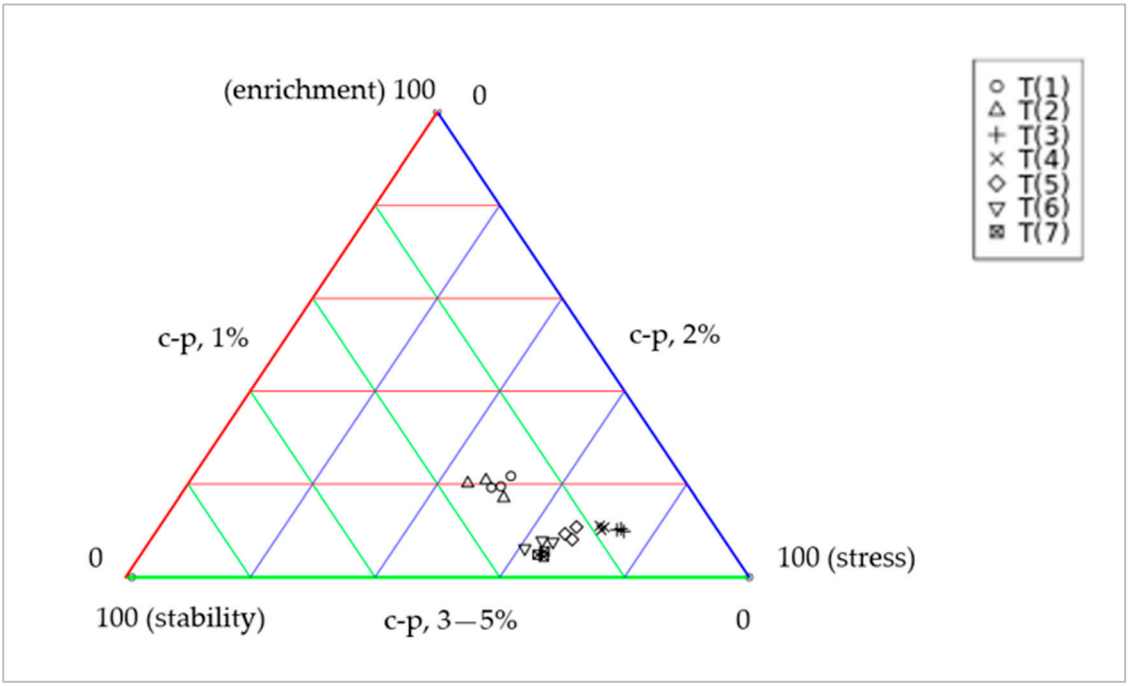


Figure 7. The ternary diagram of the experimental treatments T(1)–T(7) according to the relative contribution of c-p 1, c-p 2, and c-p 3–5 nematodes.

Plant-parasitic nematodes were dominated by c-p 2 taxa, with a maximum of 92.60 ± 1.51% in T(3). Conversely, c-p 3 taxa decreased from 38.40 ± 1.81% in T(1) to 7.40 ± 1.51% in T3, followed by an increase in T(5)–T(7). Overall, T3 produced the strongest shift towards c-p 2 taxa, indicating a pronounced alteration of nematode community structure under this treatment.

Compost treatments T(3) and T(4) were associated with a greater relative contribution of opportunistic c-p 2 taxa, indicative of communities responding to increased resource availability. In contrast, vermicompost treatments T(5)–T(7) exhibited a relative increase in more persistent c-p 3–5 taxa. Collectively, these patterns indicate a transition from a community characterized by a stronger response to resource enrichment towards a more persistent and comparatively stable community structure under vermicompost amendment (Figure 7).

Diversity metrics reflected strong shifts in community evenness caused by organic amendments (Table 4). Although species richness remained constant across all treatments (Taxa_S = 18), the Shannon diversity index (H′) was lower in T(3) (1.877 ± 0.009, $p < 0.05$) and T(4) (2.169 ± 0.019), compared to the unamended peat control T(1) (2.665 ± 0.023) and T(2) (2.510 ± 0.010; Table 4). The vermicompost treatments restored diversity, with T(6) achieving an H′ value of 2.445 ± 0.034. This suppression of diversity in T(3) was driven by a rise in dominance (Simpson Dominance, D = 0.243 ± 0.003 in T(3) vs. 0.082 ± 0.003 in T(1); $p < 0.05$), primarily reflecting the massive outbreak of *Aphelenchus* spp. and *Coslenchus* spp. (Table 4).

Soil food web diagnostics demonstrated profound functional reorganizations of the soil nematode assemblages across the experimental amendment gradient (Table 5). The maturity status of the nematode communities was significantly depressed in the high-compost variants, with the Maturity Index (MI) dropping to 2.20 ± 0.01 in T(3) and 2.25 ± 0.01 in T(4) ($p < 0.05$), which reflects the extensive proliferation of opportunistic, fast-reproducing colonizers (c-p 1,2). Concurrently, the Plant Parasitic Index (PPI) reached its minimum in T(3) (2.07 ± 0.02) and its maximum in the unamended control T(1) (2.38 ± 0.02) (Table 5).

Table 4. Nematode taxon richness, dominance, evenness and diversity indices across experimental treatments T(1)–T(7) (mean ± sd). Tukey-HSD post-hoc test ($n = 3$) expressing significant differences among the tested treatments. Means with the same superscript small letter (a, b, c) are not significantly different ($p < 0.05$).

Index Name	Treatments						
	T(1)	**T(2)**	**T(3)**	**T(4)**	**T(5)**	**T(6)**	**T(7)**
Taxa_S	18	18	18	18	18	18	18
Simpson Dominance_D	0.082 ± 0.003 g	0.098 ± 0.001 f	0.243 ± 0.003 a	0.178 ± 0.003 b	0.144 ± 0.001 c	0.12 ± 0.005 e	0.133 ± 0.004 d
Shannon_H	2.665 ± 0.023 a	2.510 ± 0.010 b	1.877 ± 0.009 f	2.169 ± 0.019 e	2.351 ± 0.005 d	2.445 ± 0.034 c	2.384 ± 0.011 cd

Table 5. Nematode community indices, food web condition indices, faunal metabolic footprints and total nematode biomass across experimental treatments T(1)–T(7), (mean ± sd). Tukey's -HSD post-hoc test ($n = 3$) expressing significant differences among the tested treatments. Means with the same superscript small letter (a, b, c, d, e, f) are not significantly different ($p < 0.05$).

Index Name	Treatments						
	T(1)	**T(2)**	**T(3)**	**T(4)**	**T(5)**	**T(6)**	**T(7)**
Maturity Index	2.38 ± 0.06 b	2.45 ± 0.04 ab	2.20 ± 0.01 c	2.25 ± 0.01 c	2.37 ± 0.04 b	2.51 ± 0.06 a	2.55 ± 0.02 a
Plant Parasitic Index	2.38 ± 0.02 a	2.27 ± 0.03 b	2.07 ± 0.02 d	2.19 ± 0.02 c	2.30 ± 0.01 b	2.33 ± 0.01 ab	2.29 ± 0.05 b
Channel Index	33.69 ± 2.08 c	34.34 ± 4.08 c	63.27 ± 0.90 ab	60.28 ± 1.39 b	61.85 ± 3.41 b	66.60 ± 2.19 ab	74.91 ± 2.11 a
Basal Index	17.43 ± 0.55 c	16.40 ± 1.80 c	30.19 ± 0.33 a	28.37 ± 0.27 a	25.90 ± 0.52 b	23.69 ± 0.98 b	24.41 ± 0.48 b
Enrichment Index	70.75 ± 0.45 a	70.93 ± 2.40 a	59.84 ± 0.35 b	60.14 ± 0.32 b	59.53 ± 1.41 bc	57.87 ± 1.00 bc	54.94 ± 0.76 c
Structure Index	69.80 ± 1.98 ab	72.70 ± 2.94 a	45.11 ± 0.88 f	50.39 ± 0.68 e	58.10 ± 1.65 d	64.81 ± 2.60 bc	65.24 ± 0.78 c
Total biomass (mg)	0.73 ± 0.11 d	2.66 ± 0.25 b	3.90 ± 0.29 a	4.62 ± 0.19 a	2.56 ± 0.15 bc	2.25 ± 0.12 bc	1.49 ± 0.16 c
Composite footprint	127.30 ± 13.75 d	426.93 ± 37.76 b	705.94 ± 43.88 a	796.79 ± 35.95 a	438.52 ± 24.95 b	361.55 ± 18.22 bc	244.02 ± 23.40 c
Enrichment footprint	42.11 ± 3.01 c	112.67 ± 12.53 b	248.82 ± 15.26 a	247.89 ± 14.90 a	119.05 ± 14.25 b	63.39 ± 9.18 c	40.58 ± 6.00 c
Structure footprint	79.48 ± 14.85 d	305.21 ± 30.12 c	416.97 ± 31.63 b	516.27 ± 19.93 a	300.88 ± 20.14 c	283.75 ± 9.28 c	193.36 ± 18.35 c
Herbivore footprint	3.63 ± 0.76 f	4.70 ± 0.11 ef	30.87 ± 1.23 a	19.50 ± 0.52 b	11.65 ± 1.02 c	10.02 ± 0.64 cd	6.68 ± 0.81 de
Fungivore footprint	4.04 ± 0.28 f	11.01 ± 0.14 e	70.80 ± 4.10 a	63.18 ± 1.91 b	32.03 ± 1.58 c	20.88 ± 1.37 d	16.90 ± 0.75 d
Bacterivore footprint	40.15 ± 3.59 c	106.01 ± 12.67 b	187.30 ± 10.49 a	197.83 ± 14.51 a	93.97 ± 12.98 b	46.89 ± 7.55 c	27.08 ± 5.03 c
Predator footprint	5.55 ± 0.56 c	12.68 ± 1.82 bc	29.17 ± 6.59 a	33.32 ± 3.46 a	29.33 ± 0.98 a	27.07 ± 4.90 a	22.15 ± 2.35 ab
Omnivore footprint	73.93 ± 14.37 d	292.53 ± 31.33 bc	387.80 ± 37.84 ab	482.95 ± 16.48 a	271.55 ± 19.23 c	256.68 ± 14.12 c	171.21 ± 19.95 c

Functional food web indices revealed marked shifts in decomposition pathways and food web stability. The Channel Index (CI) increased from 33.69 ± 2.08% in T(1) and 34.34 ± 4.08% in T(2), which indicated a bacteria-dominated decomposition channel to over 60% in T(3)–T(6), attaining its highest value in T(7) (74.91 ± 2.11%, $p < 0.05$), thereby confirming a clear transition toward fungal-mediated organic matter decomposition in compost- and vermicompost-treated substrates. The Basal Index (BI) was lowest in T(2) (16.40 ± 1.80) and T(1) (17.43 ± 0.55), but increased substantially in the amended compost treatments T(3) (30.19 ± 0.33) and T(4) (28.37 ± 0.27), before stabilizing at moderate levels (23.69-25.90) across vermicompost variants T(5)–T(7). Conversely, the Enrichment Index (EI) remained highest in the baseline substrates T(1) (70.75 ± 0.45) and T(2) (70.93 ± 2.40), declining to intermediate values in T(3)–T(6) (57.87– 60.14) and reaching its lowest level in T(7) (54.94 ± 0.76). The Structure Index (SI) showed a marked decline in compost-amended substrates, falling precipitously from 72.70 ± 2.94 in T(2) and 69.80 ± 1.98 in T(1) to an absolute minimum in T(3) (45.11 ± 0.88) and T(4) (50.39 ± 0.68, $p < 0.05$). Vermicompost incorporation supported significant structural restoration of the food web, with the SI rebounding to 64.81 ± 2.60 in T(6) and 65.24 ± 0.78 in T(7) (Table 5).

Total nematode faunal biomass varied significantly across treatments, peaking in the high-dose compost variants T(4) (4.62 ± 0.19 mg) and T(3) (3.90 ± 0.29 mg). These values represented a more than five- to six-fold increase relative to the unamended peat

control T(1) (0.73 ± 0.11 mg, $p < 0.05$). In vermicompost-treated substrates faunal biomass exhibited moderate, intermediate values, decreasing gradually from 2.56 ± 0.15 mg in T(5) and 2.25 ± 0.12 mg in T(6) to 1.49 ± 0.16 mg in T(7). Overall, while the heavy input of green waste compost T(3) and T(4) stimulated substantial biomass expansion, it compromised ecosystem stability by driving the soil food web toward an opportunist-dominated, structurally depleted state; conversely, moderate vermicompost incorporation, particularly T(6), preserved a relatively high faunal biomass while maintaining a mature, structured, and functionally balanced soil food web (Table 5).

Compost amendment ((T2)–T(4)) was associated with increasing community-level and trophic footprints, whereas increasing thevermicompost proportion (T(5)–T(7)) generally resulted in lower footprint values. The strongest responses to compost were observed for the composite, structure, bacterivore and omnivore footprints, while herbivore and fungivore footprints showed maximum values at the intermediate (50%) compost level.

The EI-SI analysis (Figure 8) demonstrates that amendment type and application rate influenced the functional development of the food web. An increased compost proportion was associated with reduced structural development, whereas vermicompost maintained higher SI values despite a gradual decline in enrichment. These contrasting responses indicate that compost and vermicompost differentially affected the balance between resource enrichment and trophic structure within the food web.

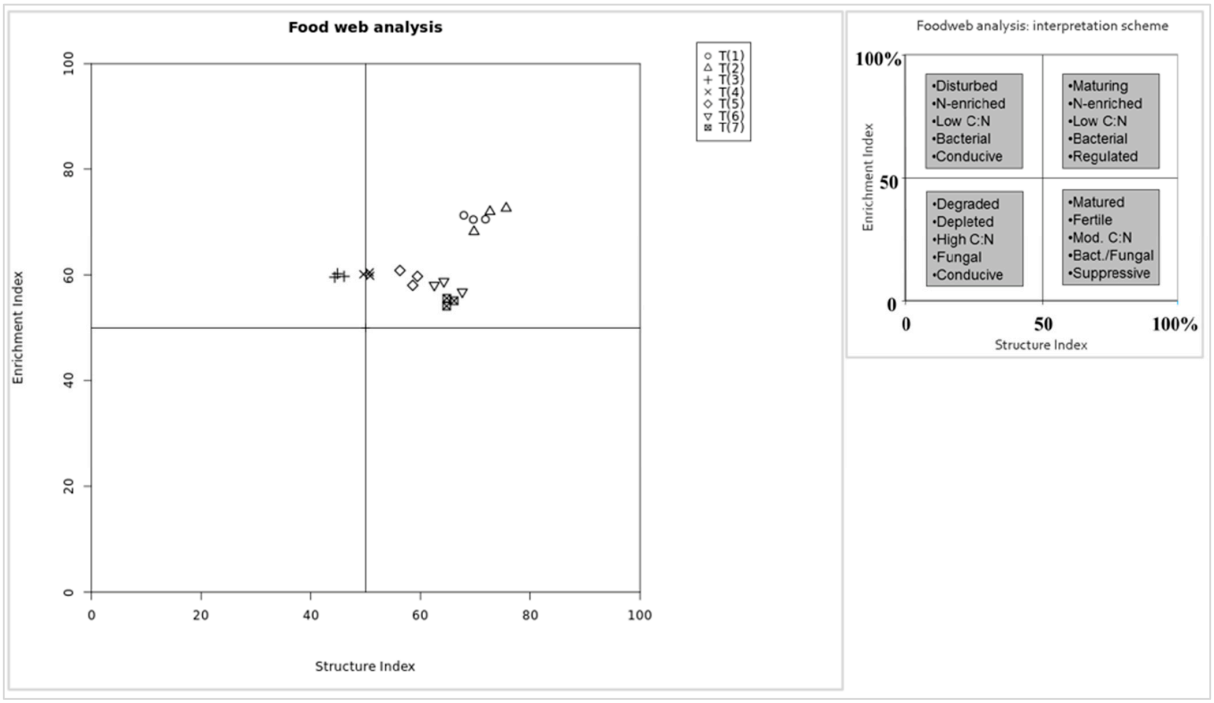


Figure 8. Plots of enrichment vs. structure indices connected with T(1)–T(7), ($n = 3$).

The correlation analysis revealed strong positive relationships between the investigated trophic groups and soil nutrient status. Bacterivores exhibited the strongest positive relationships with N-NH4 (r = 0.888), K (r = 0.887), B (r = 0.880), Zn (r = 0.842), Mg (r = 0.841), Cu (r = 0.757), Ca (r = 0.765), and P (r = 0.757). Their relationship with C org was negative (r = −0.657), while correlations with Na and Fe were weak (r = −0.066 and r = 0.277, respectively) (Figure 9). Following FDR correction using the Benjamini–Hochberg method at a significance level of α = 0.05, statistically significant associations were found for 13 out of the 17 analyzed variables. Statistical significance was observed for pH,

N-NH_4, P, K, Mg, Ca, Cu, Zn, B, Corg, S-SO_4, Mn, and NaCl. In contrast, Cl, Fe, N-NO_3, and Na did not show statistically significant results after correction for multiple comparisons.

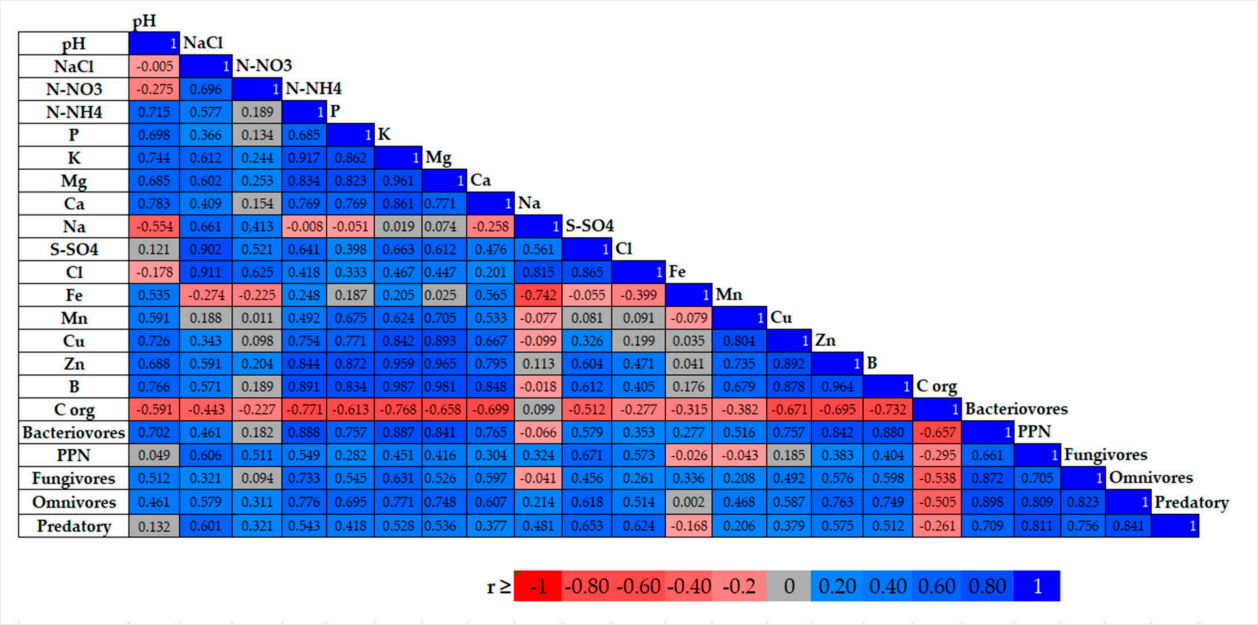


Figure 9. Pearson correlation coefficients between the selected parameters of the analyzed traits. Correlation coefficient (r) scale: −1.0: perfect negative correlation; −0.80 to −0.60: strong negative correlation; −0.40 to −0.20: moderate negative correlation; 0: no correlation; 0.20 to 0.40: moderate positive correlation; 0.60 to 0.80: strong positive correlation; 1.0: perfect positive correlation, $p \leq 0.05$.

Fungivores showed a comparable but generally weaker nutrient-related pattern, with positive correlations with N-NH_4 (r = 0.788), K (r = 0.699), B (r = 0.663), Zn (r = 0.644), Ca (r = 0.621), and P (r = 0.580), and a negative correlation with C org (r = −0.570) (Figure 9). Following FDR correction using the Benjamini–Hochberg method at a significance level of $\alpha = 0.05$, statistically significant associations were found for 11 out of the 17 analyzed variables. Statistical significance was observed for K, Ca, N-NO3, Fe, Zn, Cu, Mg, Corg, Na, Cl, and pH. In contrast, N-NH4, S-SO_4, Mn, NaCl, P, and B did not show statistically significant associations after correction for multiple comparisons.

Omnivores were also positively associated with the nutrient gradient, particularly N-NH4 (r = 0.776), K (r = 0.771), Mg (r = 0.748), B (r = 0.749), Zn (r = 0.763), and P (r = 0.695), while their correlation with C org was negative (r = −0.505) (Figure 9). After adjusting for multiple testing using the Benjamini–Hochberg FDR procedure ($\alpha = 0.05$), 14 out of the 17 investigated physicochemical parameters remained statistically significant. These included N-NH_4, P, K, Mg, Zn, B, S-SO_4, Ca, Cu, NaCl, Cl, Corg, Mn, and pH. The remaining parameters (N-NO3, Na, and Fe) did not retain statistical significance after FDR correction.

PPN exhibited positive correlations with several soil chemical properties, including N-NH4 (r = 0.604), Ca (r = 0.515), P (r = 0.449), Zn (r = 0.431), and Fe (r = 0.398). In contrast to the originally reported values, correlations with NaCl (r = 0.134), S-SO4 (r = 0.258), Cl (r = 0.078), and N-NO_3 (r = −0.022) were weak or negligible. Predatory nematodes showed positive correlations with NaCl (r = 0.601), S-SO_4 (r = 0.653), Cl (r = 0.624), and Na (r = 0.481), whereas their correlation with Fe was weak and negative (r = −0.168). The Benjamini–Hochberg procedure for controlling the false discovery rate (FDR) at a significance level of 0.05 revealed no statistically significant associations among the 17 physicochemical parameters analyzed. Although N-NH_4 showed a significant result

prior to adjustment ($p = 0.004$), this significance was not retained after FDR correction (adjusted $p = 0.068$). Thus, none of the investigated parameters remained statistically significant following correction for multiple comparisons.

For Predatory, following, Benjamini–Hochberg FDR correction ($\alpha = 0.05$) identified significant associations for 8 of the 17 physicochemical parameters: S-SO_4, Cl, NaCl, Zn, N-NH_4, Mg, K, and B. The remaining parameters were not statistically significant after correction for multiple testing.

To further assess the relationships among the investigated soil, plant, and trophic-group variables, a principal component analysis (PCA) was performed (Figure 10). The first principal component (Factor 1) explained 47.39% of the total variance, whereas the second component (Factor 2) accounted for a further 29.32%. Together, the two components explained 76.71% of the total variability, indicating that the ordination provided a good representation of the structure of the original dataset.

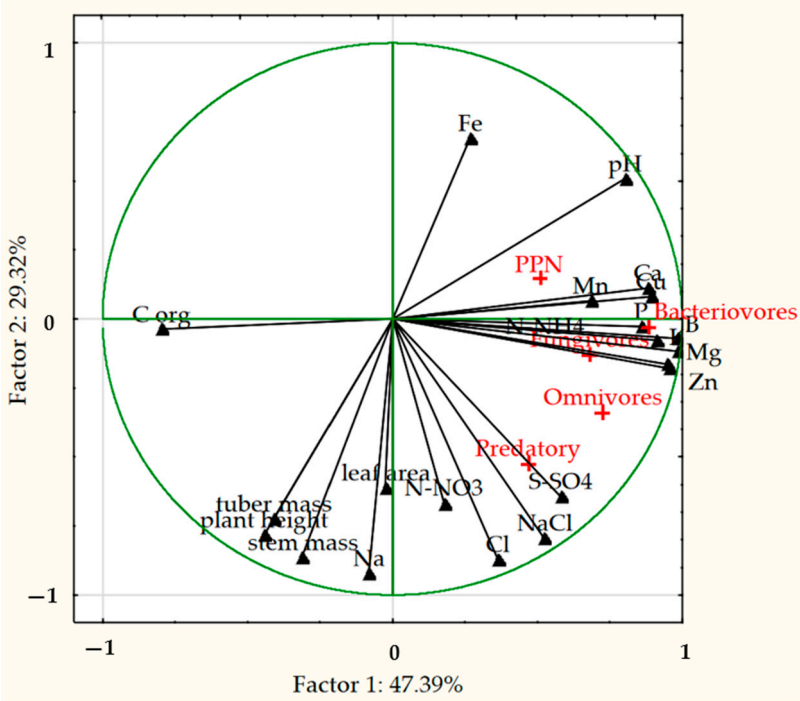


Figure 10. Principal component analysis (PCA) biplot of the distribution of the analyzed parameters.

Factor 1 primarily separated organic carbon (Corg) and plant biometric traits, including stem mass, tuber mass, plant height, and leaf area, from soil mineral and elemental variables, particularly Ca, Cu, Mn, Fe, Mg, Zn, Na, Cl, NaCl, S-SO_4, and N-NO_3. Factor 2 further differentiated variables associated with Fe and pH from salinity-related parameters. The distribution of trophic groups in the ordination space indicated their differentiation along these environmental gradients. Bacterivores and Fungivores were located on the positive side of Factor 1, whereas Predatory and Omnivores occupied lower positions along Factor 2. The PCA demonstrated that the variability in the investigated trophic groups was associated with a distinct gradient of soil chemical properties and plant characteristics, with mineral and salinity-related parameters contributing to their differentiation.

The PCA results were consistent with the analysis of variance (ANOVA), which revealed significant differences among the experimental groups in most of the investigated soil chemical properties, plant biometric traits, and nematode trophic groups ($p < 0.05$). In particular, significant differences were observed in soil pH, salinity (NaCl), nutrient concentrations, and the concentrations of several macro- and micronutrients. Plant height,

fresh biomass, tuber mass, and leaf area also differed significantly among the groups. Furthermore, all investigated nematode trophic groups, including bacterivores, fungivores, plant-parasitic nematodes (PPN s), omnivores, and predators, showed significant between-group variation. Among the nematode trophic groups, the strongest between-group differentiation was observed for PPN s ($F = 701.865$) and fungivores ($F = 544.258$), followed by bacteriovores ($F = 118.990$), omnivores ($F = 76.708$), and predatory ($F = 21.915$). These results indicate substantial variation in nematode trophic-group abundance among the experimental groups. Taken together, the PCA and ANOVA results suggest that the variation in nematode trophic groups occurred alongside differences in soil chemical properties and plant characteristics.

4. Discussion

The effects of organic amendments on plant growth depend on several interacting factors, including their chemical composition, nutrient availability, and influence on the physical and biological properties of the growing substrate. Therefore, differences in the nutrient content of amendments do not necessarily translate directly into differences in plant performance [39,40].

In our experiment, despite the lower contents of phosphorus, potassium, and trace elements in the vermicompost treatments (T(5)–T(7)) compared with the compost treatments (T(2)–T(4)), plant growth was comparable between the two amendment types. This suggests that plant performance was not determined solely by the total nutrient content of the amendments. Other factors, such as nutrient availability and the physical and biological properties of the amended substrates, may also have contributed to the observed plant growth.

The use of nematode communities as indicators is particularly relevant in managed soils, where changes in nutrient inputs and physicochemical conditions can affect the functioning of the entire soil food web [41]. The results of the present study indicate that the effects of organic amendments on substrate functioning depend not only on nutrient availability but also on the interactions between substrate chemical properties, nematode community structure, and plant physiological performance. The type and application rate of the amendments shaped substrate properties, which may have influenced both nematode communities and plant responses. In turn, changes in nematode community composition may have reflected differences in resource availability and soil food-web functioning. These findings highlight the importance of considering the interactions between substrate properties, soil biota, and plant responses when assessing the effects of organic amendments.

The similar distribution patterns of nematode trophic groups and soil nutrients indicate an association between soil nutrient status and nematode community structure. Previous studies have shown that fertilization practices and nitrogen availability are related to changes in nematode community composition [42,43]. These relationships reflect, in part, the role of microbial resources in supporting bacterivorous and fungivorous nematodes, as well as the contribution of nematodes to nutrient cycling and plant nutrient uptake [44]. Soil nutrient conditions are also relevant to plant-parasitic nematodes because host plant growth and root development determine the availability of resources for these groups. Differences in the abundance and distribution of nematode trophic groups may therefore reflect the combined effects of soil nutrient status, microbial food resources, and plant-related factors [45]. These findings support the use of nematode trophic groups as indicators of biological responses to changes in soil conditions.

The Maturity Index (MI) and Channel Index (CI) differed among treatments, describing distinct features of nematode community responses to substrate conditions. Refs. [14,36] described MI as a measure of the life-history strategies of free-living nematode communities

and their sensitivity to environmental disturbances. MI values were lowest in treatments T(3) and T(4), ranging from 2.20 to 2.25, whereas the highest values occurred in T(6) and T(7) (2.51–2.55). By comparison, CI was higher in T(7) (74.91) than in T(1) (33.69), reflecting a greater relative contribution of fungal-mediated decomposition to organic matter breakdown [16]. Although these patterns may be related to variations in substrate properties, neither NaCl concentration nor pH was consistently associated with either index. These patterns may reflect the combined influence of substrate chemical properties and resource availability on nematode life-history strategies and decomposition pathways, rather than salinity alone.

The contrasting responses of T(4) and T(6) provide particularly strong evidence for this multidimensional nature of soil fertility: the treatment characterized by the greatest nutrient enrichment did not produce the highest plant productivity, whereas a treatment with more moderate nutrient concentrations supported the most favorable photosynthetic performance and biomass accumulation. These findings highlight the importance of evaluating amendment effects through the simultaneous consideration of soil chemistry, belowground trophic organization, and plant functional responses.

Organic amendments markedly reorganized the nematode community, demonstrating a strong biological response to changes in soil resource conditions. The highest nematode abundances occurred in T(3) and T(4), with T(3) showing a particularly pronounced fungivore component and T(4) supporting high abundances across several trophic groups. The strong representation of fungivores under these treatments points to an enhanced role of the fungal-based decomposition pathway, whereas the simultaneous response of bacterivores, fungivores, omnivores, predators, and plant-parasitic nematodes under T(4) reflects broad activation of the soil food web. Such responses are consistent with the established role of nematode communities as integrative indicators of resource availability and trophic interactions [46]. Importantly, however, the magnitude of nematode abundance did not correspond directly to plant performance, indicating that biological activation of the soil food web and improved soil–plant functioning are not necessarily synonymous.

This distinction becomes particularly evident from the trophic structure and EI–SI relationships. In T(4), fungivores accounted for 66% of the community, compared with 60% in T(6), while T(6) showed a greater relative contribution of plant-parasitic nematodes, omnivores, and predators and a lower contribution of bacterivores. Thus, although T(4) supported a highly abundant nematode community, T(6) displayed a more evenly distributed trophic structure. The high Omnivore and Predator footprints recorded under T(4) further demonstrate the intensity of the trophic response, but these metrics should be interpreted as evidence of functional activation rather than as direct indicators of food-web maturity or stability. This interpretation is supported by the EI–SI analysis, in which T(4) combined strong enrichment and structural footprints with comparatively lower maturity and structural indices. The data therefore distinguish between a soil food web responding strongly to resource enrichment and one exhibiting a more balanced trophic organization.

The observed biological responses should be interpreted in the context of substrate chemical properties. Treatment T(4) had the highest concentrations of P, K, Mg, Ca, Mn, Cu, Zn, and B, as well as high concentrations of ammonium and sulfate. At the same time, it exhibited the highest NaCl, sulfate, and chloride concentrations and the highest soil pH. Increasing compost proportions affected not only nutrient availability but also the overall chemical properties of the growing substrate. The differences in Cu and Zn between T(4) and T(6) may have contributed to the contrasting biological responses, although their concentrations alone are unlikely to explain the observed patterns [47–50]. More importantly, the results point towards the combined influence of nutrient enrichment and ionic conditions rather than a single chemical driver. The PCA reinforces this interpretation

by showing that the treatments occupied distinct fertility profiles rather than forming a simple gradient of increasing nutrient availability.

The divergence between soil enrichment and plant performance was particularly pronounced under T(4). Despite having the highest concentrations of numerous mineral nutrients, T(4) did not produce the greatest tuber or stem biomass and was characterized by the least favorable PSII fluorescence parameters. Fv/Fm and Fv/F0 reached only 0.772 ± 0.047 and 3.618 ± 0.826, respectively, while the treatment also exhibited the largest area above the fluorescence curve and an increased Tfm. Collectively, these responses indicate altered PSII fluorescence kinetics and reduced photochemical efficiency. Although fluorescence parameters alone cannot identify a specific mechanism, their consistent shift under T(4) demonstrates that the highly enriched soil environment was associated with impaired functioning of the photosynthetic apparatus. The elevated abundance of *Aphelenchoides* represents an additional biotic component of the T(4) response, but the present experiment does not permit its independent contribution to be quantified.

In contrast, T(6) exhibited a distinctly different relationship between substrate properties and plant performance. It combined lower concentrations of several mineral nutrients with the highest nitrate concentration (49.66 mg kg^{-1}), very low ammonium concentration (0.55 mg kg^{-1}), and the most favorable physiological performance. Net CO_2 assimilation reached 15.72 ± 1.80 µmol CO_2 m^{-2} s^{-1}, while Fv/Fm and Fv/F0 reached 0.832 ± 0.003 and 4.966 ± 0.146, respectively. These physiological responses were accompanied by the highest tuber mass, fresh stem mass, and dry stem mass. The convergence of photosynthetic efficiency and biomass accumulation provides strong evidence that plant performance was determined by the integrated chemical environment rather than by the absolute concentration of individual nutrients. In particular, the contrasting N forms between T(4) and T(6) emphasize that nutrient availability should be considered in terms of balance and form, rather than total concentration alone. The observed changes in nematode communities following compost amendment are consistent with the findings of Milkereit et al. [51] who showed that organic amendments can strongly alter bacterial and nematode communities and affect nitrogen availability and plant growth. Their results indicated that compost stimulated bacterial groups involved in the decomposition of complex carbon compounds, while changes in microbial communities were reflected in nematode indicators of nutrient processing. Importantly, compost alone reduced plant growth in their greenhouse experiment, suggesting that the effects of organic amendments depend on substrate quality and C ratio. These findings support the importance of considering both nutrient availability and biological soil processes when evaluating the effects of compost on plant growth.

The comparison with T(7) highlights the distinction between vegetative growth and overall plant productivity, as this treatment produced the tallest plants and the greatest leaf area. However, its net photosynthetic rate was lower than in T(6), and tuber and stem biomass were also slightly lower. Greater leaf area did not necessarily result in higher carbon assimilation or biomass production, particularly when photosynthetic rates per unit leaf area differed between treatments. The lack of significant differences in stomatal conductance and transpiration among treatments means that the higher CO_2 assimilation rate in T(6) was likely related to factors other than stomatal regulation alone. Instead, the fluorescence data point to differences in the functional capacity of the photosynthetic apparatus as an important component of the treatment response.

The relationship between the nematode community and plant physiology provides an additional indication of the complexity of amendment effects. Higher nematode abundance was associated with lower PSII photochemical efficiency, with T(4) providing the clearest example of this pattern. The treatment that generated the strongest enrichment response and one of the most pronounced nematode responses simultaneously exhibited the weakest

PSII performance Environmental stress can alter both the intensity and kinetics of chlorophyll fluorescence induction, providing information on disturbances in the photosynthetic apparatus [52–55]. This apparent decoupling is important because it demonstrates that intensified belowground biological activity does not necessarily translate into improved plant functioning. Nematode-based indicators therefore provide information complementary to plant physiological measurements: they capture changes in resource enrichment and trophic organization that cannot be inferred from plant performance alone. The reduced PSII performance in T(4) may therefore reflect the combined effects of elevated nutrient and soluble ion concentrations. The high abundance of *Aphelenchoides* may have represented an additional biotic factor, as plant-associated nematodes can affect plant tissues and interfere with water and nutrient uptake. Nematodes may either suppress or facilitate plant performance depending on their trophic interactions and environmental conditions [56]. Thus, the physiological response observed in T(4) may result from the combined influence of soil chemical properties and biotic components of the soil community.

Organic carbon provides another link between the chemical and biological dimensions of the response. T(5), T(6), and T(7) maintained relatively high Corg concentrations, whereas T(4) had the lowest Corg despite its exceptionally high mineral nutrient concentrations. The opposing positioning of Corg and major mineral variables in the PCA indicates that amendment treatments generated qualitatively different soil fertility configurations. Such differences are likely to affect microbial resource pathways and, consequently, the trophic groups that depend on them. Thus, the biological response of the soil cannot be interpreted independently of both nutrient availability and the organic resource base supporting microbial activity.

The predominance of opportunistic c-p 2 taxa under the higher compost treatments is consistent with previous studies showing that organic enrichment can stimulate rapid increases in bacterial-feeding, enrichment-opportunistic nematodes. Bongiorno et al. [20] showed that nematode abundance and diversity, as well as indices such as MI, EI, and SI, reflect different aspects of soil food web functioning, indicating that nematode abundance alone is insufficient to assess food web quality or stability. Steel et al. [57] likewise reported that organic enrichment initially favors opportunistic bacterial feeders, whereas substrate maturation is accompanied by shifts in trophic composition, including increased contributions from fungivores and higher trophic groups. These findings are consistent with the nematode community responses to compost amendments observed in the present study.

Taken together, the results challenge a unidimensional view of soil fertility in which higher nutrient concentrations are assumed to represent improved soil conditions. In T(4), high nutrient concentrations and nematode abundance were not accompanied by better plant performance, as photosynthetic activity and biomass production remained comparatively low. In contrast, T(6) combined lower concentrations of several nutrients with favorable nitrogen availability, a more evenly distributed nematode trophic structure, efficient PSII functioning, high CO_2 assimilation, and the greatest tuber and stem biomass. Differences between these treatments reflect the combined roles of chemical enrichment, nutrient form, ionic conditions, organic carbon content, and biological organization in shaping the effects of organic amendments. From an agronomic perspective, these findings emphasize that the response to organic amendments should be evaluated beyond nutrient accumulation in soil.

A treatment can strongly stimulate belowground biological activity while simultaneously imposing chemical conditions that constrain plant physiological performance. Conversely, a less strongly enriched environment can support more efficient resource use and greater biomass production when nutrient availability and soil biological functioning are better balanced. The integrated assessment of nematode trophic structure, EI–SI

characteristics, soil chemistry, chlorophyll fluorescence, gas exchange, and plant biomass therefore provides a more functionally informative framework for evaluating amendment effects than any individual indicator. In the present study, the strongest biological enrichment and the strongest plant response occurred under different amendment conditions, demonstrating that soil food-web activation and plant productivity represent related but distinct dimensions of soil functioning.

Compost can improve soil properties and plant growth [39,58]; however, higher application rates do not necessarily result in better plant performance. Excessive application may negatively affect plant growth, partly due to increased concentrations of soluble salts. These findings highlight the importance of using moderate vermicompost rates to achieve optimal plant growth and yield.

5. Conclusions

Compost amendments altered soil properties, nematode community structure, and the physiological performance of Jerusalem artichoke. Nematode trophic structure provides complementary indicators of soil–plant functioning that capture compost-induced changes beyond conventional measures of soil fertility and crop productivity. Integrating soil chemical properties, nematode-based indicators, and plant physiological responses provides a more comprehensive assessment of compost effects. These findings demonstrate that both chemical and biological soil functioning are critical for understanding compost impacts on plant performance.

Supplementary Materials: The following supporting information can be downloaded at: https://www.mdpi.com/article/10.3390/agriculture16222536/s1, Figure S1: Jerusalem artichoke (*Helianthus tuberosus* L.) plants 7 weeks after planting under different substrate treatments T(1)–T(7). T(1) vs. T(2) (A); T(1) vs. T(3) (B); T(1) vs. T(4) (C); T(1) vs. T(5) (D); T(1) vs. T(6) (E); T(1) vs. T(7) (F).

Author Contributions: Conceptualization, A.Z. and W.J.; methodology, W.J., A.T.S., D.K. and M.K.; formal analysis, A.Z.; investigation, A.Z., W.J., A.T.S., D.K. and M.K.; resources, A.T.S. and M.K.; writing—original draft preparation, A.Z.; writing—review and editing, A.Z.; visualization, A.Z. and D.K. All authors have read and agreed to the published version of the manuscript.

Funding: This research is funded by financial resources of the Ministry of Science and Higher Education for scientific activities of the Institute of Agricultural Sciences, Land Management and Environmental Protection, University of Rzeszów.

Institutional Review Board Statement: Not applicable.

Data Availability Statement: The original contributions presented in this study are included in the article. Further inquiries can be directed to the corresponding author.

Conflicts of Interest: The authors declare no conflicts of interest.

References

1. Penuelas, J.; Coello, F.; Sardans, J. A better use of fertilizers is needed for global food security and environmental sustainability. *Agric. Food Secur.* **2023**, *12*, 5. [CrossRef]
2. Chen, J.; Mola, M.; Liu, X.; Lee, T.M.; Monokrousos, N.; Veresoglou, S.D. Cost–benefit analysis across smallholder rice farmers reveals that fertilization practices severely compromise their income. *Agric. Res.* **2025**, *15*, 1460–1468. [CrossRef]
3. Xu, Q.; Ling, N.; Chen, H.; Duan, Y.; Wang, S.; Shen, Q.; Vandenkoornhuyse, P. Long-Term Chemical-Only Fertilization Induces a Diversity Decline and Deep Selection on the Soil Bacteria. *mSystems* **2020**, *5*, e00337-20. [CrossRef] [PubMed]
4. Li, K.; Chen, A.; Sheng, R.; Hou, H.; Zhu, B.; Wei, W.; Zhang, W. Long-term chemical and organic fertilization induces distinct variations of microbial associations but unanimous elevation of soil multifunctionality. *Sci. Total Environ.* **2024**, *931*, 172862. [CrossRef] [PubMed]
5. Chen, H.; Shi, X.; Yang, H.; Wang, X.; Li, H. Soil nematodes as bioindicators of agricultural management practices: Insights from bibliometric analysis. *Environ. Sustain. Indic.* **2026**, *29*, 101123. [CrossRef]

6. Hammerschmiedt, T.; Kintl, A.; Holatko, J.; Mustafa, A.; Vitez, T.; Malicek, O.; Baltazar, T.; Elbl, J.; Brtnicky, M. Assessment of digestates prepared from maize, legumes, and their mixed culture as soil amendments: Effects on plant biomass and soil properties. *Front. Plant Sci.* **2022**, *13*, 1017191. [CrossRef] [PubMed]
7. Massalha, N.; Plewa, M.J.; Nguyen, T.H.; Dong, S. Influence of anaerobic mesophilic and thermophilic digestion on cytotoxicity of swine wastewaters. *Environ. Sci. Technol.* **2020**, *54*, 3032–3038. [CrossRef] [PubMed]
8. Holatko, J.; Hammerschmiedt, T.; Kucerik, J.; Kintl, A.; Baltazar, T.; Malicek, O.; Latal, O.; Brtnicky, M. Fertilisation of permanent grasslands with digestate and its effect on soil properties and sustainable biomass production. *Eur. J. Agron.* **2023**, *149*, 126914. [CrossRef]
9. Dominati, E.; Patterson, M.; Mackay, A. A framework for classifying and quantifying the natural capital and ecosystem services of soils. *Ecol. Econ.* **2010**, *69*, 1858–1868. [CrossRef]
10. Garrigues, E.; Corson, M.S.; Angers, D.A.; van der Werf, H.M.G.; Walter, C. Soil quality in life cycle assessment: Towards development of an indicator. *Ecol. Indic.* **2012**, *18*, 434–442. [CrossRef]
11. Harris, J. Soil microbial communities and restoration ecology: Facilitators or followers? *Science* **2009**, *325*, 573–574. [CrossRef] [PubMed]
12. Kapp, C.; Storey, S.G.; Malan, A.P. Options for soil health measurement in vineyards and deciduous fruit orchards, with special reference to nematodes. *S. Afr. J. Enol. Vitic.* **2013**, *34*, 272–280. [CrossRef]
13. Knox, O.; Polain, K.; Fortescue, E.; Griffiths, B. Distribution and Restricted Vertical Movement of Nematodes in a Heavy Clay Soil. *Agronomy* **2020**, *10*, 221. [CrossRef]
14. Bongers, T.; Ferris, H. Nematode community structure as a bioindicator for environmental monitoring. *Trends Ecol. Evol.* **1999**, *14*, 224–228. [CrossRef] [PubMed]
15. Neher, D.A. Role of nematodes in soil health and their use as indicators. *J. Nematol.* **2001**, *33*, 161–168. [PubMed]
16. Ferris, H.; Matute, M.M. Structural and functional succession in the nematode fauna of a soil food web. *Appl. Soil Ecol.* **2003**, *23*, 93–110. [CrossRef]
17. Ferris, H. Form and function: Metabolic footprints of nematodes in the soil food web. *Eur. J. Soil Biol.* **2010**, *46*, 97–104. [CrossRef]
18. Sánchez-Moreno, S.; Nicola, N.L.; Ferris, H.; Zalom, F.G. Effects of agricultural management on nematode-mite assemblages: Soil food web indices as predictors of mite community composition. *Appl. Soil Ecol.* **2009**, *41*, 107–117. [CrossRef]
19. Du Preez, G.; Daneel, M.; De Goede, R.; Du Toit, M.J.; Ferris, H.; Fourie, H.; Geisen, S.; Kakouli-Duarte, T.; Korthals, G.; Sánchez-Moreno, S.; et al. Nematode-based indices in soil ecology: Application, utility, and future directions. *Soil Biol. Biochem.* **2022**, *169*, 108640. [CrossRef]
20. Bongiorno, G.; Bodenhausen, N.; Bünemann, E.K.; Brussaard, L.; Geisen, S.; Mäder, P.; Quist, C.W.; Walser, J.C.; de Goede, R.G.M. Reduced tillage, but not organic matter input, increased nematode diversity and food web stability in European long-term field experiments. *Mol. Ecol.* **2019**, *28*, 4987–5005. [CrossRef] [PubMed]
21. Mola, M.; Nikolaidou, C.; Valerin, M.C.; Campanaro, S.; Papatheodorou, E.M.; Mylonas, I.; Aschonitis, V.; Monokrousos, N.; Kougias, P.G. Linking anaerobic digestate application to soil microbial and nematode. *Appl. Soil Ecol.* **2026**, *222*, 107038. [CrossRef]
22. Grabau, Z.J.; Chen, S. Influence of long-term corn–soybean crop sequences on soil ecology as indicated by the nematode community. *Appl. Soil Ecol.* **2016**, *100*, 172–185. [CrossRef]
23. Nowosielski, O. *Zasady Opracowywania Zaleceń Nawozowych w Ogrodnictwie. Wyd. III uzupełnione*; PWRiL: Warszawa, Poland, 1988; p. 310. Available online: https://w.bibliotece.pl/402626/Zasady%20opracowywania%20zalece%C5%84%20nawozowych%20w%20ogrodnictwie (accessed on 31 August 2026). (In Polish)
24. Komosa, A.; Breś, W.; Golcz, A.; Kozik, E. *Żywienie Roślin Ogrodniczych—Podstawy i Perspektywy*; Państwowe Wydawnictwo Rolnicze i Leśne (PWRiL): Poznań, Poland, 2012; p. 390. Available online: https://www.agroswiat.pl/zywienie-roslin-ogrodniczych-11920.html (accessed on 31 August 2026). (In Polish)
25. Ostrowska, A.; Gawliński, S.; Szczubiałka, Z. *Metody Analizy i Oceny Właściwości Gleb i Roślin*; Instytut Ochrony: Warszawa, Poland, 1991; p. 334. Available online: https://www.scirp.org/reference/referencespapers?referenceid=1394461 (accessed on 31 August 2026). (In Polish)
26. Antweiler, R.C.; Patton, C.J.; Taylor, H.E. *Automated Colorimetric Methods for Determination Nitrate Plus Nitrite, Nitrite, Ammonium and Orthophosphate Ions in Natural Water Samples*; U.S. Geological Survey: Reston, VA, USA, 1996. [CrossRef]
27. Zawadzińska, A.; Salachna, P.; Nowak, J.S.; Kowalczyk, W.; Piechocki, R.; Łopusiewicz, Ł.; Pietrak, A. Compost Based on Pulp and Paper Mill Sludge, Fruit-Vegetable Waste, Mushroom Spent Substrate and Rye Straw Improves Yield and Nutritional Value of Tomato. *Agronomy* **2022**, *12*, 13. [CrossRef]
28. Regulation (EU) 2019/1009 of the European Parliament and of the Council. 2019. Available online: http://data.europa.eu/eli/reg/2019/1009/oj (accessed on 31 August 2026).
29. Easlon, H.M.; Bloom, A.J. Easy Leaf Area: Automated digital image analysis for rapid and accurate measurement of leaf area. *Appl. Plant Sci.* **2014**, *2*, 1400033. [CrossRef] [PubMed]
30. Szczygieł, A. Application of the Centrifugal Method for Extraction of Nematodes from Soil. *J. Prog. Agric. Sci.* **1971**, *12*, 169–179.

31. Brzeski, M.W. Nematodes of Tylenchina in Poland and Temperate Europe. In *Muzeum i Instytutu Zoologii*; Polska Akademia Nauk (MiIZ PAN): Warsaw, Poland, 1998; ISBN 83-85192-84-0.
32. Andrássy, I. Free-Living Nematodes of Hungary (Nematoda Errantia). In *Pedozoologica Hungarica*; Csuzdi, C., Mahunka, S., Eds.; Hungarian Natural History Museum and Systematic Zoology Research Group of the Hungarian Academy of Sciences: Budapest, Hungary, 2007; Volume II, ISBN 963 7093 98 2.
33. Stefanovska, T.; Skwiercz, A.; Pidlisnyuk, V.; Zhukov, O.; Kozacki, D.; Mamirova, A.; Newton, R.A.; Ust'ak, S. The Short-Term Effects of Amendments on Nematode Communities and Diversity Patterns under the Cultivation of Miscanthus × giganteus on Marginal Land. *Agronomy* **2022**, *12*, 2063. [CrossRef]
34. Yeates, G.W.; Bongers, T.; De Goede, R.G.M.; Freckman, D.W.; Georgieva, S.S. Feeding Habits in Soil Nematode Families and Genera—An Outline for Soil Ecologists. *J. Nematol.* **1993**, *25*, 315–331. [PubMed]
35. Hammer, O.; Harper, D.; Ryan, P. PAST: Paleontological Statistics Software Package for Education and Data Analysis. *Palaeontol. Electron.* **2001**, *4*, 4.
36. Bongers, T. The Maturity Index: An Ecological Measure of Environmental Disturbance Based on Nematode Species Composition. *Oecologia* **1990**, *83*, 14–19. [CrossRef] [PubMed]
37. Ferris, H.; Bongers, T.; de Goede, R.G.M. A Framework for Soil Food Web Diagnostics: Extension of the Nematode Faunal Analysis Concept. *Appl. Soil Ecol.* **2001**, *18*, 13–29. [CrossRef]
38. Sieriebriennikov, B.; Ferris, H.; de Goede, R.G.M. NINJA: An Automated Calculation System for Nematode-Based Biological Monitoring. *Eur. J. Soil Biol.* **2014**, *61*, 90–93. [CrossRef]
39. Lim, S.L.; Wu, T.Y.; Lim, P.N.; Shak, K.P.Y. The use of vermicompost in organic farming: Overview, effects on soil and economics. *J. Sci. Food Agric.* **2015**, *95*, 1143–1156. [CrossRef] [PubMed]
40. Blouin, M.; Barrere, J.; Meyer, N.; Lartigue, S.; Barot, S. Vermicompost significantly affects plant growth. A meta-analysis. *Agron. Sustain. Dev.* **2019**, *39*, 34. [CrossRef]
41. Lu, Q.; Liu, T.; Wang, N.; Dou, Z.; Wang, K.; Zuo, Y. A review of soil nematodes as biological indicators for the assessment of soil health. *Front. Agric. Sci. Eng.* **2020**, *7*, 275–281. [CrossRef]
42. Pan, F.; McLaughlin, N.B.; Yu, Q.; Xue, A.G.; Xu, Y.; Han, X.; Li, C.; Zhao, D. Responses of soil nematode community structure to different long-term fertilizer strategies in the soybean phase of a soybean–wheat–corn rotation. *Eur. J. Soil Biol.* **2010**, *46*, 105–111. [CrossRef]
43. Wei, C.; Zheng, H.; Li, Q.; Lü, X.; Yu, Q.; Zhang, H.; Chen, Q.; He, N.; Kardol, P.; Liang, W.; et al. Nitrogen addition regulates soil nematode community composition through ammonium suppression. *PLoS ONE* **2012**, *7*, e43384. [CrossRef] [PubMed]
44. Gebremikael, M.T.; Steel, H.; Buchan, D.; Bert, W.; De Neve, S. Nematodes enhance plant growth and nutrient uptake under C- and N-rich conditions. *Sci. Rep.* **2016**, *6*, 32862. [CrossRef] [PubMed]
45. Burkhardt, A.; Briar, S.; Martin, J.M.; Carr, P.M.; Sherman, J. Characterization of soil nematode community structure in semi-arid dryland barley systems. *Agrosyst. Geosci. Environ.* **2022**, *5*, e20277. [CrossRef]
46. Forge, T.; Hogue, E.; Neilsen, G.; Neilsen, D. Effects of organic mulches on soil microfauna in the root zone of apple: Implications for nutrient fluxes and functional diversity of the soil food web. *Appl. Soil Ecol.* **2003**, *22*, 39–54. [CrossRef]
47. Nieboer, E.; Richardson, D.H.S. The Replacement of the Nondescript Term 'Heavy Metals' by a Biologically and Chemically Significant Classification of Metal Ions. *Environ. Pollut. Ser. B Chem. Phys.* **1980**, *1*, 3–26. [CrossRef]
48. Sochova, I.; Hofman, J.; Holoubek, I. Using Nematodes in Soil Ecotoxicology. *Environ. Int.* **2006**, *32*, 374–383. [CrossRef] [PubMed]
49. Korthals, G.W.; van de Ende, A.; van Megen, H.; Lexmond, T.M.; Kammenga, J.E.; Bongers, T. Short-Term Effects of Cadmium, Copper, Nickel and Zinc on Soil Nematodes from Different Feeding and Life-History Strategy Groups. *Appl. Soil Ecol.* **1996**, *4*, 107–117. [CrossRef]
50. Chauvin, C.; Trambolho, M.; Hedde, M.; Makowski, D.; Cérémonie, H.; Jimenez, A.; Villenave, C. Soil Nematodes as Indicators of Heavy Metal Pollution: A Meta-Analysis. *Open J. Soil Sci.* **2020**, *10*, 579–601. [CrossRef]
51. Milkereit, J.; Geisseler, D.; Lazicki, P.; Settles, M.L.; Durbin-Johnson, B.P.; Hodson, A. Interactions between nitrogen availability, bacterial communities, and nematode indicators of soil food web function in response to organic amendments. *Appl. Soil Ecol.* **2021**, *157*, 103767. [CrossRef]
52. Kalaji, M.H.; Łoboda, T. Photosystem II of barley seedlings under cadmium and lead stress. *Plant Soil Environ.* **2007**, *53*, 511–516. [CrossRef]
53. Kuckenberg, J.; Tartachnyk, I.; Noga, G. Temporal and spatial changes of chlorophyll fluorescence as a basis for early and precise detection of leaf rust and powdery mildew infections in wheat leaves. *Precis. Agric.* **2009**, *10*, 34–44. [CrossRef]
54. Murkowski, A.; Mila, A. Wpływ podwyższonego stężenia CO_2 na fluorescencję chlorofilu i fotosyntezę wybranych genotypów rzepaku ozimego [The effect of increased CO_2 concentration in atmosphere on chlorophyll fluorescence and photosynthesis of some genotypes of winter oilseed rape]. *Rośl. Oleiste Oilseed Crops* **2010**, *31*, 283–292.

55. Mikiciuk, M.; Malinowska, K.; Wróbel, J.; Ptak, P.; Studziński, M.; Rokosa, M. Effects of 2-hydroxybenzoic acid on the efficiency of the photosynthetic apparatus of basket willow (*Salix viminalis* L.) plant growing under conditions of salt stress. *Folia Pomer. Univ. Technol. Stetin. Agric. Aliment. Pisc. Zootech.* **2017**, *338*, 109–118. [CrossRef]
56. Topalović, O.; Geisen, S. Nematodes as suppressors and facilitators of plant performance. *New Phytol.* **2023**, *238*, 2305–2312. [CrossRef] [PubMed]
57. Steel, H.; Moens, T.; Vandecasteele, B.; Hendrickx, F.; De Neve, S.; Neher, D.A.; Bert, W. Factors influencing the nematode community during composting and nematode-based criteria for compost maturity. *Ecol. Indic.* **2018**, *85*, 409–421. [CrossRef]
58. Zapałowska, A.; Jarecki, W.; Skwiercz, A.T.; Kunka, M. The Impact of Using Compost, Vermicompost and Mineral Fertilization on Soil Nematode Communities and Maize Grain Quality in a Pot Experiment. *Sustainability* **2025**, *17*, 9936. [CrossRef]

Disclaimer/Publisher's Note: The statements, opinions and data contained in all publications are solely those of the individual author(s) and contributor(s) and not of MDPI and/or the editor(s). MDPI and/or the editor(s) disclaim responsibility for any injury to people or property resulting from any ideas, methods, instructions or products referred to in the content.